Thesis

Association between subcutaneous adipose tissue and urine metabolites in elementary school children

submitted by

Philipp Huberts

in partial fulfillment of the requirements of the degree of

Doktor der gesamten Heilkunde
(Dr. med. univ.)

at the

Medical University of Graz

executed at the
Division of Physiology and Pathophysiology

under the supervision of

Nandu Goswami, Assoz.-Prof. Priv.-Doz. Dr.med. Dr.med.univ. MMedSci PhD

and

Karin Schmid-Zalaudek, Priv.-Doz. Mag. Dr.rer.nat.

and

Hansjörg Habisch, Sen.Scientist Dr.rer.nat.

Graz, 02.09.2024

Declaration of Academic Integrity

I hereby confirm that the present diploma thesis is the result of my own independent scholarly work. I also confirm that in all cases, where material from the work of others (in books, articles, essays, dissertations, and on the internet) is acknowledged, quotations and paraphrases are clearly indicated. No material other than that cited in the reference list has been used. I have read and understood the Medical University's regulations and procedures concerning plagiarism.

Graz, 02.09.2024 *Philipp Huberts m.p.*

Acknowledgements

I would like to express my gratitude to Assoz.-Prof. Priv.-Doz. Dr. med. Dr. med. univ. MMedSci PhD Nandu Goswami, Mag. Priv.-Doz. Dr.rer.nat. Karin Schmid-Zalaudek, and Sen. Scientist Dr.rer.nat. Hansjörg Habisch for providing me with the opportunity to participate in this study, for their guidance, continuous support, and unwavering patience throughout the process of authoring this thesis, and for the extensive knowledge that I was able to accumulate in the course of this diploma thesis. I want to extend my sincerest gratitude to the team at the Division of Physiology of the Medical University of Graz, particularly Mr. Johann Wagner, BSc. Ing. Andreas Jantscher and Bakk.rer.soc.oec. Ing. Alfred Fürhapter-Rieger, whose invaluable assistance was instrumental in the collection of data for this diploma thesis.

My gratitude also extends to the children who participated in the study, as well as to the educators and principals of the participating academic institutions. Furthermore, I would like to express my gratitude to the City of Graz and ERASMUS for its financial assistance in supporting this project.

I would be remiss if I did not express my profound gratitude towards my parents, grandparents, and girlfriend for their unwavering encouragement and assistance throughout this academic journey. I am especially indebted to my brother Tobias for his invaluable expertise and guidance.

Zusammenfassung

Hintergrund: Der kontinuierliche Anstieg der Prävalenz von Adipositas bei Kindern steht mit einer Reihe von Faktoren, die zu diesem Phänomen beitragen, in Zusammenhang. Dazu gehören unter anderem der zunehmende Verzehr von zucker- und fetthaltigen Lebensmitteln sowie ein Rückgang an körperlicher Betätigung. Diese Diplomarbeit ist Teil der Studie "Health and Academic Performance with Happy Children (HAPHC)", die darauf abzielt, Fettleibigkeit bei Volksschulkindern genauer zu untersuchen und mögliche Präventionsmaßnahmen zu ermitteln.

Zielsetzung: Die vorliegende Diplomarbeit befasst sich mit den potenziellen Konsequenzen von Adipositas im Kindesalter in Bezug auf die Zusammensetzung der im Harn nachweisbaren Metaboliten. Das Ziel der vorliegenden Untersuchung bestand darin, zunächst festzustellen, welche Metaboliten im Urin von Grundschulkindern grundsätzlich zu finden sind. In einem zweiten Schritt sollten Unterschiede im Metaboliten-Profil zwischen Gruppen identifiziert werden, die anhand ihres subkutanen Fettgewebes klassifiziert wurden. Die auffälligen Metaboliten sollten anschließend anhand von Literaturrecherche genauer auf mögliche pathologische Mechanismen untersucht werden, um Rückschlüsse auf schädliche Effekte der Adipositas im Kindesalter zu erhalten.

Methode: Für die vorliegende Studie wurden die Daten von 353 gesunden Kindern im Alter von 6 bis 11 Jahren aus drei verschiedenen Volksschulen in Graz, Österreich, herangezogen. Das subkutane Fettgewebe wurde an acht standardisierten Stellen gemessen und Urinproben wurden am Morgen in jeder der teilnehmenden Schulen gesammelt. Die Metaboliten im Urin wurden mittels NMR-Spektroskopie detektiert, mit dem Ziel, 150 verschiedene Metaboliten zu identifizieren. Das subkutane Fett wurde mittels Bright-mode Ultraschall gemessen, um die Dicke dessen an acht verschiedenen Regionen zu bestimmen. Die Kinder wurden dann auf Basis ihres Anteils an subkutanem Fett (Summe des subkutanen Fettes an acht Stellen) anhand der Terzile in drei gleiche Gruppen eingeteilt. Mittels Hauptkomponentenanalyse (PCA) wurden relevante Urinmetaboliten identifiziert, und mittels ANOVA wurden die Kreatinin-normalisierten Urinmetaboliten der drei Gruppen vergleichen, wobei die False Discovery Rate (FDR) zur Korrektur der p-Werte verwendet wurde.

Ergebnisse:

Von den 150 untersuchten Urinmetaboliten konnten 83 im Harn der untersuchten Kinder nachgewiesen werden. Besonders erwähnenswert ist, dass in 22% der Proben Glucose nachgewiesen werden konnte. Ebenso konnten Unterschiede im Metaboliten-Profil der Kinder bezüglich Geschlecht, Größe, Gewicht und BMI festgestellt werden. Darüber hinaus wurde festgestellt, dass Mädchen im Durchschnitt mehr subkutanes Fett aufwiesen als Jungen. Die auf Basis des SAT klassifizierten Gruppen wiesen signifikante Unterschiede in Bezug auf das Auftreten von Allantoin auf ($F_{(1, 35)} = 9{,}362$, $p = 0{,}002$, $p_{corr.} = 0{,}034$), wobei die höchsten Konzentrationen in der Gruppe mit niedrigem Anteil an subkutanem Fett beobachtet wurden. Ein ähnliches Muster konnte für Bernsteinsäure beobachtet werden, für die ein signifikanter Unterschied zwischen Kindern mit wenig subkutanem Fett und jenen mit viel, nachgewiesen wurde ($F_{(1, 35)} = 9{,}757$, $p = 0{,}002$, $p_{corr.} = 0{,}034$). Die niedrigsten Konzentrationen wurden bei Kindern mit hohem subkutanem Fett beobachtet. Die beobachteten Unterschiede für Glycin ($F_{(1, 351)} = 4{,}836$, $p = .029$, $p_{corr.} = .41$) und Ethylmalonsäure ($F_{(1, 351)} = 4{,}441$, $p = .036$, $p_{corr.} = .43$) blieben jedoch nach Korrektur der p-Werte (FDR) nicht signifikant.

Schlussfolgerung: Diese Diplomarbeit zeigt auf, dass sich die Metaboliten im Urin von Kindern mit hohem Anteil an subkutanen Fettgeweben von jenen mit niedrigem Anteil durchaus unterscheiden. Im Rahmen der vorliegenden Untersuchungen konnten insgesamt drei Metaboliten identifiziert werden, nämlich Bernsteinsäure, Allantoin und Glycin, welche im Kontext von Adipositas bei Kindern von Relevanz sein könnten, wobei diesen Metaboliten eine Vielzahl von Funktionen im menschlichen Körper zukommt. Die Diagnose von Fettleibigkeit durch einen Urintest könnte in Zukunft eine nicht-invasive Option für die frühzeitige Erkennung von Adipositas und damit assoziierten Erkrankungen bei Kindern darstellen. Allerdings ist weitere Forschung erforderlich, um exakte Kriterien zu definieren.

Abstract

Background: The prevalence of childhood obesity is on a persistent upward trajectory with numerous factors contributing to this phenomenon. Among other factors, the increasing consumption of sugary and fatty foods, coupled with a decline in physical activity, are significant contributors to this phenomenon. This diploma thesis is part of the study "Health and Academic Performance with Happy Children (HAPHC)," which aims to investigate obesity in elementary school children in greater detail and to identify potential preventive measures.

Aims and Objectives: This diploma thesis deals with the potential effects of childhood obesity for the composition of metabolites detectable in the urine. The aim of the study was firstly to determine which urinary metabolites are generally found in the urine of elementary school children. In a second step, differences in the metabolite profile between groups classified according to their amount of subcutaneous adipose tissue (SAT) were studied, through literature research, to draw conclusions about the pathological mechanisms of childhood obesity.

Methods: For the present study, data of 353 healthy children aged 6 to 11 years from three different elementary schools in Graz, Austria, were included. SAT was measured at eight standardized sites and urine samples were collected during the morning hours in each of the participating schools. The urinary metabolites were subjected to nuclear magnetic resonance spectroscopy, with the objective of identifying 150 different metabolites. SAT was measured by bright-mode ultrasound, which was applied to assess the thickness of the SAT on eight different regions. The children got tercile divided into three equal groups based on the sum of the SAT at the eight sites. Principal component analyses (PCA) was performed to identify relevant urine metabolites and one-way ANOVA was calculated to compare the creatinine-normalized urinary metabolites of the three SAT groups, applying false discovery rate (FDR) for correction of p-values.

Results: Of the 150 urine metabolites tested, 83 were detected in the urine of the children examined. Of particular note was the detection of glucose in 22% of the samples. Additionally, differences were observed in the metabolite profile of the children with regard to sex, height, weight, and body mass index (BMI). The SAT tercile-based groups exhibited

significant differences with regard to allantoin ($F(1, 351) = 9.362$, $p = .002$, $p_{corr.} = .034$), with the highest concentrations observed in the group with low SAT (T1). A similar pattern was observed for succinic acid, for which a significant main effect was found ($F(1, 351) = 9.757$, $p = .002$, $p_{corr.} = .034$). The lowest concentrations were observed in children with high amounts of SAT (T3). However, the observed differences for glycine ($F(1, 351) = 4.836$, $p = .029$, $p_{corr.} = .41$) and ethylmalonic acid ($F(1, 351) = 4.441$, $p = .036$, $p_{corr.} = .43$) did not remain significant after correction of p-values.

Conclusion: The present study demonstrated that the urinary metabolites of children with high SAT differ from those with low SAT. A total of three metabolites were identified, namely succinic acid, allantoin, and glycine, which may be pertinent in the context of childhood obesity and have a variety of functions within the human body. In the future, the identification of obesity through a urine test may offer a non-invasive alternative for the early diagnosis of childhood obesity. Nevertheless, further research is required to establish precise criteria for this.

Table of contents

List of abbreviations

ALA	delta-aminolevulinic acid
ATP	adenosine triphosphate
B	circumferences of the biceps
BMI	body mass index
B-mode	brightness-mode
BR	brachioradialis
cases	children in whom a certain metabolite was found
CREA	creatinine
CS	control school
CT	computer tomography
d	distance
D_I	subcutaneous adipose tissue including the fibrous structures
DMA	dimethylamine
DNA	deoxyribonucleic acid
DT	distal triceps
DXA	dual-energy X-ray absorptiometry
EO	external oblique
ES	erector spinae
FDR	false discovery rate
FT	front thigh
h	body height
H	circumferences of the hip
HAPHC	Health and Academic Performance with Happy Children
HOPP	Health Oriented Pedagogical Project
I_1R	imidazoline I_1-receptor
IOTF	International Obesity Task Force
IS1	intervention school 1
IS2	intervention school 2
ISAK	International Society for the Advancement of Kinanthropometry
l	leg length
LA	lower abdomen

LOD	limit of detection
LT	lateral thigh
m	body mass
Max	maximum
MC	medial calf
MC4R	melanocortin 4 receptor
MELAS	Mitochondrial encephalomyopathy with lactic acidosis and stroke-like episodes
Min	minimum
MRI	magnetic resonance imaging
NMR	nuclear magnetic resonance
oPLS-DA	Orthogonal partial least squares discriminant analysis
PACC	physical activity across the curriculum
PCA	principal component analyses
POMC	proopiomelanocortin
RNA	ribonucleic acid
ROHHADNET	rapid onset obesity, hypothalamic dysfunction, hypoventilation, autonomic dysregulation and neuroendocrine tumors
s	sitting height
SAT	subcutaneous adipose tissue
SD	standard deviation
Sucnr1	succinate receptor 1
T	circumferences of the thigh
TCA	Tricarboxylic acid
UA	upper abdomen
W	circumferences of the waist
WAGR	Wilms' tumor, aniridia, genitourinary anomalies, and Retardation
WC	waist circumference
WHO	World Health Organization
WHR	waist-to-hip ratio
WHtR	waist-to-height ratio

Summary of figures

Summary of tables

1. Introduction

Overweight in children and adolescents has become a global problem in recent years. Despite efforts to counteract this trend, the number of people affected is increasing dramatically. The number of overweight children is increasing particularly in third world countries (Goswami et al., 2022, WHO, 2017, WHO, 2021). In Europe, there is also a trend towards less physical activity and sports among children and young adults. This trend is associated with an increase in the number of people who are overweight and who will later face the consequences of obesity (Goswami et al., 2022, Sturm et al., 2020).

The objective of the Happy Children Study was to provide an empirical basis for understanding the rising prevalence of childhood obesity and its associated health and social consequences. Furthermore, the study aimed to identify evidence-based strategies for addressing this public health concern. This diploma thesis, as part of the Happy Children Study, specifically addresses the relationship between obesity, as assessed through measurement of subcutaneous adipose tissue (SAT), and its effects on urine composition, analyzed by nuclear magnetic resonance (NMR) spectroscopy.

1.1 Anatomy of fat

The adipose tissue of the human body can be subdivided into two distinct categories: white adipose tissue and brown adipose tissue (see Figure 1). These entities exhibit distinct functional and structural characteristics.

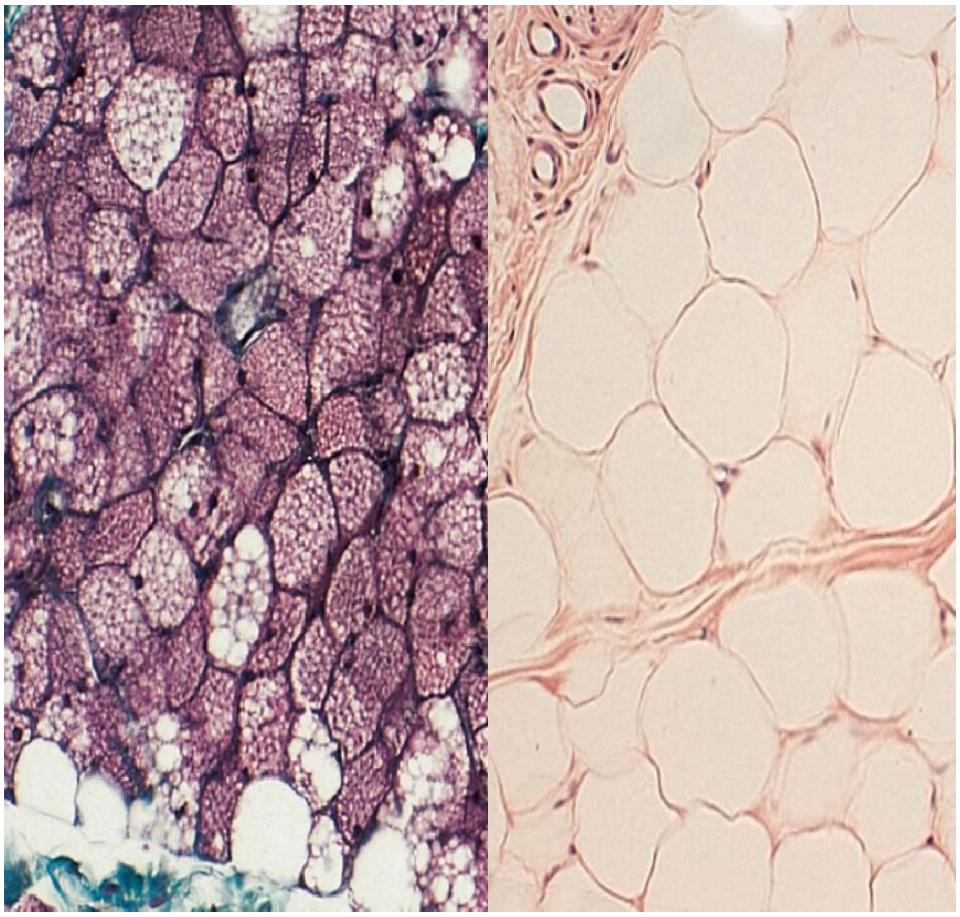

Figure 1: Comparison of brown and white adipose tissue.
Left: Brown fatty tissue in Goldner's stain (Welsch et al., 2022)
Right: White adipose tissue (kerosene embedded)in hematoxylin eosin stain (Lüllmann-Rauch and Paulsen, 2019)

The cells of the white adipose tissue (adipocytes) consist mostly of a fat droplet, which displaces the cytoplasm along with the cell organelles and the nucleus to the plasma membrane. The intake of fat occurs in the form of fatty acid and glycerol into the adipocyte via pinocytosis. The necessary substances for this process are delivered to the adipocyte via the blood. An alternative method for the filling of the adipocyte with fat is the synthesis of fatty acids and glycerol by the cell itself from glucose (Anderhuber et al., 2012). The majority of fat is accumulated as triglyceride, which is constructed out of glycerin and a trivalent alcohol, to which three fatty acids are attached. Triglycerides are the most efficient

energy storage per unit of mass in the human body, with capacity to release 39kJ/mol of energy when burned. Additionally, triglycerides serve a variety of functions, including insulation in subcutaneous fat, as structural fat and organ fat, as seen in the kidney capsule (Horn et al., 2015).

In instances of extreme starvation, the body is also capable of utilizing structural fat, which is typically found in the sole of the foot or behind the eyeball, as an energy source. If the body requires the production of energy from the fat deposit, the adipocyte separates little fat droplets from the fat vacuole. The fat is then divided at the plasmalemma into fatty acids and glycerol and subsequently transported through the intercellular space into the blood (Anderhuber et al., 2012). Fatty tissue is characterized by a robust vascular supply, which enables it to undergo continuous remodeling even when energy intake is maintained at a stable level. Another crucial attribute of fatty tissue is its substantial capacity to retain water. This property plays a pivotal role in maintaining the body's water and salt balance (Anderhuber et al., 2012). Adipocytes are clustered together in fat lobules, which are vascularized independently and surrounded by collagen fibers. When subjected to mechanical stress, collagen fibers exhibit the ability to return to their original position once the deforming forces are removed. Therefore, adipose tissue fulfills also a cushioning function (Anderhuber et al., 2012).

The white adipose tissue can be distinguished according to its localization into two distinct categories: visceral fat and subcutaneous fat. Although the study situation is not entirely clear, it seems reasonable to assume that the proportion of total body fat accounted for by visceral fat is about 10-20% in men and 5-8% in women. The proportion of visceral fat is observed to increase with age, regardless of sex (Mohsen, 2009, Wajchenberg, 2000, Arner, 1997).

Subcutaneous and visceral adipose tissue not only differ in localization, but also show differences in their composition. Subcutaneous adipose tissue is composed of smaller adipocytes, which influences its metabolic profile. These smaller adipocytes demonstrate higher insulin sensitivity and a higher avidity for triglyceride and free fatty acid uptake. Furthermore, visceral adipose tissue is better vascularized and better innervated than subcutaneous adipose tissue (Mårin et al., 1992, Misra and Vikram, 2003, Mohsen, 2009).

Brown adipose tissue is composed of numerous small fat vacuoles. It is also characterized by a high density of nerves and blood vessels. The primary function of brown adipose tissue is to facilitate rapid energy provision for thermoregulation in newborns and infants (Anderhuber et al., 2012).

1.2 Etiology of Childhood Obesity

The causes of childhood obesity can be classified into two main categories: exogenous and endogenous. Exogenous causes are based on an imbalance between calorie intake and consumption, whereas endogenous causes include genetic, syndromic, and endocrine factors (Bhawana and Vandana, 2018).

1.2.1 Exogenous Obesity

Children today are exposed to a multitude of factors that contribute to the ease with which they can gain weight. However, maintaining fitness requires a sustained commitment to effort. An unhealthy lifestyle can be influenced by a number of factors, including family, school, neighborhood, the food industry, and government policy (Hill and Peters, 1998, Swinburn et al., 1999).

Individual Behaviors

A closer examination of individual behavior reveals several potential sources of risk for obesity. For example, the consumption of energy-rich foods, packaged refined foods, sugar sweetened beverages, excessive snacking, skipping meals, large portion sizes, and a low intake of fruit and vegetables represent significant sources of risk for obesity (Bowman et al., 2004). Furthermore, a lack of exercise, an increase in screen time, and a reduction in sleep duration have been linked to a negative impact on normal weight (Mamun et al., 2007, Bhawana and Vandana, 2018).

Micro-environmental Influences

In considering the micro-environmental influences, the family unit merits particular attention. The parenting style and behavior of parents, along with their dietary habits and level of physical activity, exert a pronounced influence on their children. Furthermore, there is an elevated risk of obesity in cases where the mother has diabetes, smokes, or is obese. Infant feeding practices, sleep duration, and the rate of postnatal weight gain are also

associated with an increased likelihood of obesity in later life (Johnson and Birch, 1994, Spruijt-Metz et al., 2002, Cutting et al., 1999). Schools exert a notable impact on children's health and well-being. Promoting a healthy diet and sufficient physical activity can help prevent obesity, whereas a lack of safe outdoor spaces and access to unhealthy food options in school can contribute to its prevalence (Shah et al., 2010, French and Wechsler, 2004).
A study conducted between 2021 and 2022 in Carinthia, Austria, demonstrated the importance of promoting local sports clubs to encourage children to engage in more physical activity. Additionally, the positive effects of increased physical activity in everyday school life, particularly for children who are not members of a sports club, were also evidenced (Jarnig et al., 2023). The home environment can counteract perceived obesity through the availability of healthy food and parks (Bhawana and Vandana, 2018).

Macro-environmental Influences

It would be remiss to underestimate the role of the food industry in the prevalence of childhood obesity. The production of foods high in fat, sugar and/or salt; complex marketing and advertising practices; aggressive sales tactics; and food labels that are difficult to understand collectively limit consumers' ability to make informed dietary choices (Bhawana and Vandana, 2018).The government can facilitate the reduction of childhood obesity by providing a safe environment that encourages physical activity. This could include the construction of playgrounds and open gyms, as well as the designation of bicycle- and pedestrian-friendly streets. Furthermore, the implementation of strict nutritional policies is necessary to encourage the consumption of healthy foods. This could entail the taxation of unhealthy foods, the introduction of clear food labeling, and the imposition of price controls on fruit and vegetables (Swinburn et al., 1999, Bowman et al., 2004).

1.2.2 Endogenous Obesity

Endogenous causes of childhood obesity include endocrinopathies, monogenetic syndromes, and other genetic syndromes. It is crucial to acknowledge that endogenous causes represent a significantly smaller proportion than that of exogenous causes (Bhawana and Vandana, 2018).

Endocrinopathies

Endocrinopathies are responsible for only approximately 2-3% of all cases of childhood obesity (Crino et al., 2003). However, a diagnosis of these diseases is of significant

importance for individuals affected and their families. One important indicator of an endocrinological cause is a decline or failure of linear growth, which results in a child falling below the expected growth for their genetic potential (Crocker and Yanovski, 2009, Mason et al., 2014). A number of endocrinopathies, including hypothyroidism, Cushing syndrome, growth hormone deficiency, hypothalamic obesity, Albright hereditary osteodystrophy, ROHHADNET (rapid onset obesity, hypothalamic dysfunction, hypoventilation, autonomic dysregulation and neuroendocrine tumors) syndrome, and persistent hyperinsulinemia, can lead to obesity (Bhawana and Vandana, 2018).

Monogenetic Dysfunctions

Monogenetic dysfunctions are the result of single-gene mutations that cause a defect in proteins that regulate food intake and energy consumption in the hypothalamus. Children with this type of disorder exhibit pronounced hyperphagia, which results in a rapid increase in weight during the first year of life. The underlying causes of such diseases include leptin deficiency, leptin receptor mutations, proopiomelanocortin (POMC) deficiency, preproconvertase deficiency, and, most commonly, melanocortin 4 receptor (MC4R) mutations (Farooqi and O'Rahilly, 2005, Bereket et al., 2012, Mason et al., 2014).

Syndromic Disorders

In contrast to monogenetic disorders, the excess weight associated with syndromic disorders typically develops after infancy. Examples of such disorders include Prader-Willi syndrome, Bardet-Biedl syndrome, Alström syndrome, Albright's hereditary osteodystrophy, and WAGR (Wilms' tumor, aniridia, genitourinary anomalies, and retardation) syndrome. These diseases are characterized by cognitive impairment, dysmorphic features, and organ anomalies (Mason et al., 2014).

1.3 Potential health risks associated with being overweight

The health risks associated with childhood obesity are far-reaching and extend beyond the immediate health problems that may result, such as high blood pressure, metabolic syndrome, high cholesterol levels, type 2 diabetes, orthopedic problems, sleep apnea, asthma, and fatty liver (Williams et al., 2002). As the metabolic syndrome offers a comprehensive overview of the pathological physical effects of obesity, a detailed explanation is provided below.

To date, no universally accepted definition of metabolic syndrome in children has been established. Since 2003, numerous working groups have endeavored to establish a definition of metabolic syndrome. The majority of authors have adapted the guidelines for adults in their proposed definitions. It is widely accepted that the following four criteria must be met in order to diagnose metabolic syndrome: (1) hyperinsulinemia/impaired glucose metabolism/insulin resistance, (2) arterial hypertension, (3) dyslipidemia, and (4) abdominal obesity. Nevertheless, the definitions continue to diverge with regard to the specified cut-off values. The most widely accepted definition of metabolic syndrome in children is the one proposed by Cook et al. (Cook et al., 2003) and the International Diabetes Federation (IDF) (Alberti et al., 2005), which defines metabolic syndrome as abdominal obesity and the presence of two or more typical clinical features. It is important to note that anthropometric, clinical, and metabolic parameters utilized to diagnose metabolic syndrome must be adjusted for age and sex (Weihe and Weihrauch-Blüher, 2019).

Childhood obesity is also linked to a range of psychological, social, and behavioral issues. These include reduced self-confidence, body image problems, social isolation, discrimination, and depression (Williams et al., 2002). There is compelling evidence that childhood obesity is a significant risk factor for adverse health outcomes in adulthood (Reilly and Kelly, 2011). Indeed, the ramifications of childhood obesity are so multifaceted that it is challenging to enumerate and categorize them exhaustively (Pulgarón, 2013).

1.4 Measurement of obesity

The World Health Organization (WHO) defines obesity as an excess of adipose tissue that is sufficient to elevate the risk of morbidity, alter physical, psychological, or social well-being, and/or result in mortality (WHO, 2000). Both body composition and growth rate have a significant impact on children's health. In the field of pediatrics, percentile curves are often utilized to ascertain growth, weight, and height in relation to age. Body mass index (BMI) is also a commonly employed tool for diagnosing obesity. However, these methods have limited significance (Javed et al., 2015, Okorodudu et al., 2010, Ranasinghe et al., 2021, Vanderwall et al., 2017, Adom et al., 2020). The following section will discuss various methods for determining obesity.

1.4.1 Subcutaneous Adipose Tissue (SAT) Measurement by Ultrasound

This is the methodology employed to ascertain the prevalence of overweight in this thesis. The measurement of subcutaneous fat using ultrasound has been demonstrated to be an exceptionally precise and dependable method in comparison to the considerably more costly measurement techniques such as dual-energy X-ray absorptiometry (DXA), computer tomography (CT), or magnetic resonance imaging (MRI), which necessitate an institutional setting, such as hospitals or universities (Müller et al., 2016, Müller et al., 2020, Störchle et al., 2017, Kelso et al., 2020, Wajchenberg, 2000, Simoni et al., 2020). As ultrasound measurement assesses uncompressed adipose tissue, it is possible to differentiate between an increase in body weight due to muscle growth and an increase in fat as can be seen in Figure 2 (Müller et al., 2016, Müller et al., 2020, Sengeis et al., 2019).

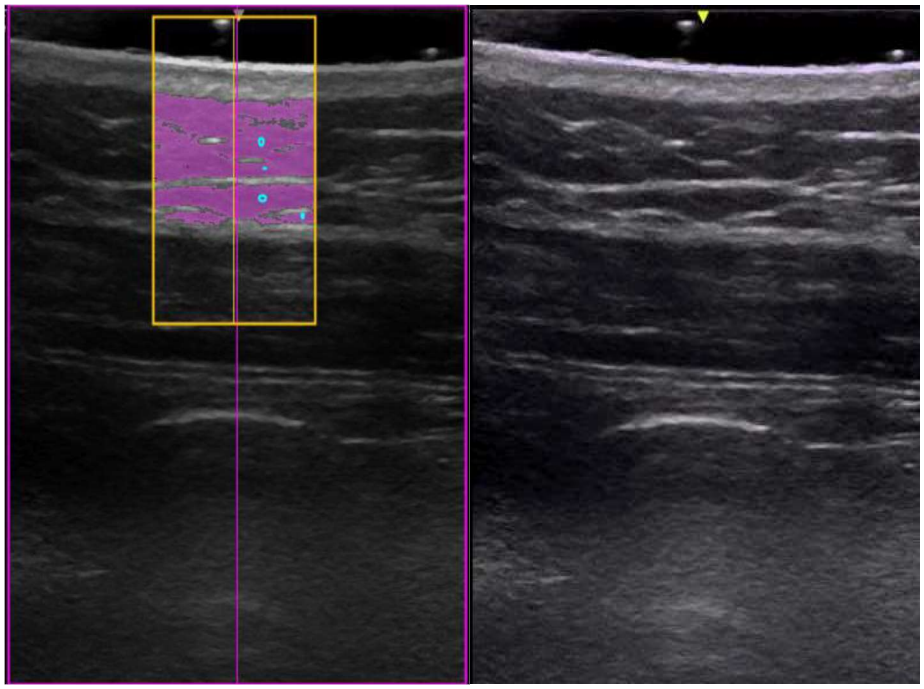

Figure 2: Ultrasound image of the subcutaneous adipose tissue.
Left: The subcutaneous adipose tissue is indicated in purple, with muscle tissue situated beneath.
Right: The same ultrasound image without marking of the SAT

Furthermore, the method has the advantage of not requiring ionized radiation for measurement, which allows for uninhibited follow-up assessments (Kelso et al., 2020, Simoni et al., 2020).

A measurement of subcutaneous fat is useful in the context of this study, as previous studies have demonstrated a correlation between elevated SAT at the waist and an increased risk of

cardiometabolic disorders, particularly in children (Ali et al., 2014, Liu et al., 2010, Kjellberg et al., 2019, Lee et al., 2017, Yan et al., 2019, Kelly et al., 2014, González-Álvarez et al., 2017, Matsha et al., 2019, Nazare et al., 2012). In a large-scale study conducted in China, the researchers measured the SAT of children and adolescents between the ages of 6 and 18 using DXA. They observed a significant correlation between elevated SAT and an increased prevalence of total cholesterol, high-density and low-density lipoprotein cholesterol, and triglycerides (Yan et al., 2019). These findings reinforce the crucial role of SAT assessment in quantifying an elevated cardiometabolic risk (Schmid-Zalaudek et al., 2021). A more comprehensive elaboration can be found in section 3.5.1 SAT -Measurement.

1.4.2 MRI and CT

MRI is a highly sophisticated and costly imaging procedure utilized in the field of medicine. The procedure necessitates the utilization of an exceedingly strong (superconducting) magnet, a magnetic field gradient system, which is indispensable for signal localization, and a radio frequency system, which is employed for signal generation and processing. The ability of MRI to differentiate between soft tissues is superior to that of CT and ultrasound. The MRI does not require the use of ionizing radiation, thus rendering the method non-invasive. The measurement of adipose tissue via MRI necessitates the utilization of a sophisticated software. The purpose of clinical software is to detect diseases; it is not designed to measure fat. Whole-body scans are feasible, but they must be recorded as a series of stacks and subsequently be integrated. Additional constraints associated with MRI-based fat measurement include the 2mm x 2mm pixel size employed in whole-body scans and the challenge of discerning between tissue layers (Ackland et al., 2012).

CT, like magnetic resonance imaging, is capable of producing high-resolution images of the interior of the body. However, in contrast to MRI, CT is associated with radiation exposure. The X-ray tube and the radiation detector rotate around the subject, enabling image reconstruction following the measured attenuation relative to air and water, quantified in Hounsfield units. However, whole-body measurements are not justifiable in the context of non-clinical application in children due to the high radiation exposure (Ackland et al., 2012), and thus not for the research question of the present thesis.

In summary, neither CT nor MRI are practical methods for measuring fat on a large scale due to the aforementioned disadvantages, especially the high technical complexity requiring institutional assessment, such as clinics or hospitals (Ackland et al., 2012).

1.4.3 Dual Energy X-Ray Absorptiometry

Dual energy x-ray absorptiometry involves sending filtered x-rays of two different photon energies through the subject, attenuating them to different degrees. The patient lies on the scanning table and the mass and composition of each pixel is recorded in relation to bone mineral, fat and fat-free soft tissue. The measurement of fat is determined by the ratio of soft tissue attenuation of the two energies, and the in vivo elemental composition supports the underlying physical concept of this being accurate (Wang et al., 2010). A potential source of error in DXA is that it assumes segmental constancy in tissue composition. However, the water and lipid content of skin, fat, muscle, and bone tissue varies regionally (Clarys et al., 2010). Another factor to consider is the radiation dose to which the subject is exposed during the examination (Ackland et al., 2012).

1.4.4 Bioelectrical Impedance Analysis

Bioelectrical impedance analysis is a technique that employs electrical impedance to calculate an individual's body composition, based on their resistance and size. The formula utilized in this process is that which determines the volume of a conductor through which an electric current of a specific frequency is passed, with consideration given to the length and resistance of the conductor in question. The fundamental tenets of this methodology are the assumption of a cylindrical conductor and the uniformity of current flow through the conductor (Chumela and Sun, 2005, Ackland et al., 2012).

In 2016, McCarthy et al. published reference curves for Caucasian children aged 5-18 years to determine overweight status using bioelectrical impedance measurement. The 85th percentile was identified as the threshold for overweight, while the 95th percentile was defined as the cutoff for obesity (McCarthy et al., 2006). Despite the prevalence of bioimpedance measurement in the field of body composition assessment, particularly for the estimation of body water and fat percentage, the accuracy of this technique has been shown to be constrained (Ackland et al., 2012, Lohman, 1992).

1.4.5 Body Mass Index and Mass Index

The Body Mass Index (BMI) is a well-established method for assessing obesity and underweight. It is calculated by dividing body weight by the square of height. However, in individuals with body composition/constitution that deviates from the norm, this can result in significant misinterpretations. One method for optimizing the BMI is to incorporate leg length and sitting height into the calculation. These values are readily accessible and could markedly enhance the precision of the assessment(Ackland et al., 2012). Furthermore, large-scale studies have demonstrated that anthropometric measurements, including waist circumference (WC), waist-to-hip ratio (WHR), and waist-to-height ratio (WHtR), can enhance the diagnosis of obesity (Fredriksen et al., 2017, Jensen et al., 2016). In conclusion, it is important to highlight that a modified BMI is not an optimal method for assessing obesity. This is because it utilizes total body mass rather than fat mass in its calculations (Ackland et al., 2012), which may also result from muscle mass. This was demonstrated in a study on preschool children in which fat mass was measured using air displacement plethysmography (Delisle Nyström et al., 2018). Sensitivity of the BMI measurement in relation to overweight is inadequate. In a quarter of cases, overweight children could not be identified as such ((Javed et al., 2015, Okorodudu et al., 2010, Adom et al., 2020, Rothman, 2008, Wickramasinghe et al., 2005).

For children, there are multiple curves that indicate the BMI cut-off for overweight and obesity based on age and sex. The most widely recognized definitions of childhood obesity are those proposed by the World Health Organization (WHO) and the International Obesity Task Force (IOTF) (Monasta et al., 2011). The IOTF employs centile curves, which correlate with BMI thresholds of 25 and 30 kg/m² at the age of 18, to delineate the parameters of overweight and obesity (Cole et al., 2000). The World Health Organization (WHO) defines children aged 0-5 years with a body mass index (BMI) or weight-for-length/height greater than two standard deviations (SD) as overweight and children with a BMI or weight-for-length/height greater than three SD as obese (WHO, 2006). For children aged 5-19 years, overweight is defined as a BMI greater than one SD and obesity as a BMI greater than two SD (Onis et al., 2007).

1.4.6 Skin fold measurement

To date, over 100 methods have been developed for calculating subcutaneous fat using skinfold measurements (Lohman et al., 1988). The inconsistent results of this method are

attributable to differences in the populations measured as well as the lack of standardization of the method. For instance, a mere 1cm alteration in the location of the skinfold measurement points can result in considerable discrepancies in the recorded data (Hume and Marfell-Jones, 2008). This underscores the necessity for a precise delineation of the measurement points. As a result, a guideline was written in Virginia in 1986 in the course of a national standardization conference (Lohman et al., 1988). At the same time the International Society for the Advancement of Kinanthropometry (ISAK) was founded in Glasgow, which developed an examination-based certificate and a precisely defined protocol for measuring skin folds (Marfell-Jones et al., 2006). The application of both guidelines resulted in a notable enhancement in the precision of the measurement outcomes (Ackland et al., 2012).

The skinfold measurement was typically validated with densitometry to ascertain its accuracy. In certain instances, a measurement inaccuracy exceeding 3% was identified, with some general equations exhibiting an even higher inaccuracy of 5%. This level of inaccuracy is deemed unacceptable for measurement purposes (Durnin and Womersley, 1974, Ackland et al., 2012). Additional sources of error in skinfold measurement include the assumption of a constant dermal and epidermal thickness, a uniform compressive capacity of subcutaneous adipose tissue at all measurement points, a uniform relative fat distribution, a constant proportion of fat in adipose tissue, and a constant ratio of internal to external adipose distribution. Additionally, the assumed constancy of fat-free mass density may introduce error. The resulting error in accurately estimating the percentage of body fat necessarily includes the additional errors of the reference method (usually densitometry) (Ackland et al., 2012).

1.5 Anatomy of the urinary system

The kidneys are approximately 10-12 cm in length, 6 cm in width, 4 cm in thickness and weigh about 160 grams. There is considerable variation in the size, shape and position of the kidneys among individuals. Each kidney is coated by a capsula fibrosa, a capsula adiposa and a fascia renalis. In most cases, the left kidney is longer, thicker and heavier than the right kidney. The kidneys extend from approximately the twelfth thoracic vertebra to the third lumbal vertebra, situated on either side of the spine within the lumbar fossa. The kidney is internally divided into two distinct regions: the renal medulla and the renal

cortex. The renal medulla is composed of seven to fourteen pyramids, the tips of which project into the renal calyces. Each pyramid is circumscribed by a cortical mantle, which forms a renal lobe with it. The renal cortex is a layer of tissue measuring 5-7 mm in thickness, situated beneath the renal capsule. The fundamental structural units of the kidney are the nephrons. There are approximately 2.5 million nephrons in the kidneys collectively. Each nephron is comprised of a renal corpuscle and the associated tubular system, including the proximal, intermediate and distal tubules. The connecting segment leads to the collecting duct, which in turn merge into the ducts of Bellini, which empty into the renal calyces. The renal pelvic caliceal system and the ureter constitute the urinary tract, which leads the urine into the bladder from where it is excreted via the urethra (Anderhuber et al., 2012). Figure 3 summarizes the discussed anatomy of the urinary system for a better understanding.

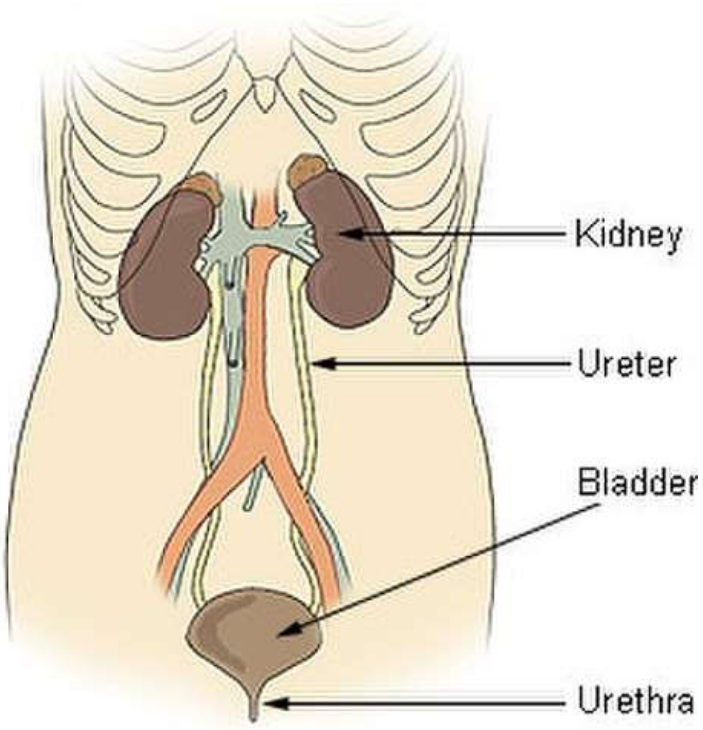

Figure 3:The urinary system
Source: https://commons.wikimedia.org/w/index.php?search=urinary+system&title=Special:MediaSearch&go=Go&type=image&haslicense=unrestricted

1.6 Urine formation

The formation of urine is primarily accomplished through filtration in the glomeruli. This process is driven by the pressure exerted by the blood within the glomerular capillaries,

which forces the primary urine out of the glomerular capillaries. Substances are transported from the tubular lumen into the peritubular capillaries and subsequently back into the blood along the tubule. This transport is facilitated by diffusion processes as well as active transport mechanism. However, in addition to reabsorbing substances, tubular cells can also actively secrete them in the opposite direction. This means that, aside from macromolecules, the glomerular filtrate contains all substances dissolved in the plasma, and in a concentration that is virtually identical to that of plasma water. Figure 4**Fehler! Verweisquelle konnte nicht gefunden werden.** depicts the filtration function of the kidney.

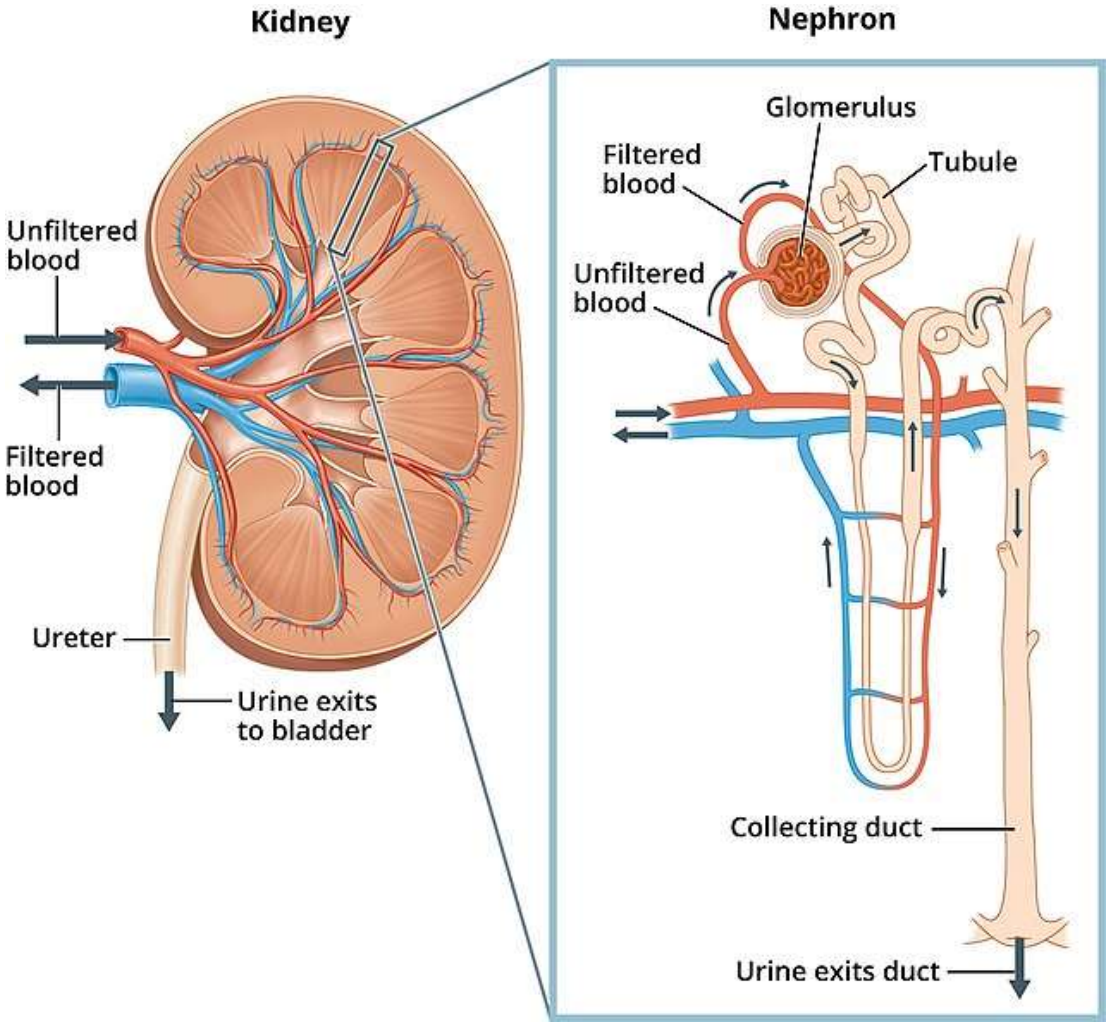

Figure 4: Urine formation
Source: https://commons.wikimedia.org/w/index.php?search=kidney&title=Special:MediaSearch&go=Go&type=image&haslicense=unrestricted

The combined daily glomerular filtration rate of kidneys is approximately 180 liters, with a substantial quantity of dissolved substances being filtered out. The combination of filtration rate and varying degrees of reabsorption of different substances ultimately determines the

composition of the urine. Metabolic end products, such as creatinine, sulfate and urea, that must be excreted can be eliminated in large amounts. In contrast, the excretion of water and electrolytes can be adjusted to a greater extent depending on the body's needs (Pape et al., 2014).

Following its passage through the renal tubules, which are approximately 3-4 cm in length, the primary urine is subjected to reabsorption, with approximately 99% of it being reabsorbed. The color of the urine ranges from light yellow to dark red and is determined by the presence of urochrome and urobilinogen (Anderhuber et al., 2012).

1.7 Urine Metabolomics

In a broader sense, the origins of metabolomics testing can be traced back to ancient Greece, where urine was evaluated based on its color, taste, and smell to diagnose diabetes (Goh et al., 2007). The initial systematic studies were conducted in the 1970s by Hornig and Hornig (Horning and Horning, 1971b, Horning and Horning, 1971a) as well as by Pauling et al. (Pauling et al., 1971). These studies initially focused on the comprehensive state-specific metabolite set in biological fluids, rather than on the determination of individual metabolites.

Over the past two years, the modern approach to metabolomics has undergone significant developments. This refers to a systematic and comprehensive quantification of small molecule metabolites (i.e., molecules weighing less than 1500 Daltons) in biological samples at a specific point in time. As with the genome and proteome, the metabolome is defined as the set of all metabolites present in a cell, tissue, organ, or organism at a given state. (Bujak et al., 2015).

Metabolomics can provide insights into the research of therapeutic effects, the pathogenesis of diseases, and the identification of biomarkers for obesity (Wei et al., 2012, Lu et al., 2016, Bujak et al., 2015, Kim et al., 2011). Several, studies have already been conducted on animals with high-fat diet-induced obesity, in which a metabolomic profile was created using nuclear magnetic resonance or liquid chromatography-mass spectrometry (Kim et al., 2011, Shearer et al., 2008, Kim et al., 2009, Liu et al., 2012). Using animal whole blood and liver tissue samples, abnormalities in fatty acid metabolism, lipid metabolism, and amino acid metabolism were detected, and some biomarkers in urine were identified that may be

associated with obesity (Men et al., 2017).Elliot et al. employed 24-hour urine samples to ascertain the metabolic profile of individuals with obesity, utilizing proton (1H) nuclear magnetic resonance (NMR) spectroscopy and ion exchange chromatography. The researchers identified 29 molecular species, which are interconnected within metabolic pathways, as being significantly associated with BMI. Among the identified metabolites were urinary glycoproteins and N-acetylneuraminate (related to renal function), trimethylamine, dimethylamine, 4-cresyl sulfate, phenylacetylglutamine, and 2-hydroxyisobutyrate (gut microbial co-metabolites), succinate, and citrate. Tricarboxylic acid cycle intermediates, ketoleucine, and the ketoleucine/leucine ratio (which are linked to skeletal muscle mitochondria and branched-chain amino acid metabolism), ethanolamine (which is involved in skeletal muscle turnover), and 3-methylhistidine (which is linked to skeletal muscle turnover and meat intake) were also identified (Elliott et al., 2015).

To date only a few studies concerning the urine metabolome of children have been conducted. In a study published in 2015 examining the gut microbiome of children and its impact on obesity, NMR-based analysis of urinary metabolites revealed diet-related changes in the metabotype of overweight children (Zhang et al., 2015). In 2018, NMR spectroscopy of urine was used to detect a decrease in trimethylamine N-oxide levels, a risk factor for cardiovascular disease, in obese prepubertal children. To this end, 34 prepubertal children completed a 6-month intervention program based on nutritional advice according to the Mediterranean diet and WHO recommendations. Anthropometric, metabolic and nutritional variables were recorded before and after the intervention (Leal-Witt et al., 2018). Lee et al. collected anthropometric/biochemical data and fasting serum, urine, and fecal samples from children at baseline and after an eight-week weight-loss lifestyle modification program to examine the gut microbiome and its metabolites for an effect on obesity. It was found that lifestyle changes leading to weight loss were associated with changes in fatty acid biosynthesis and myristic acid (Lee et al., 2023). A previous study by Liu et al. employed liquid chromatography coupled with high-resolution mass spectrometry to examine urinary metabolites. In this study, 348 children and 315 adults, aged between 1 and 78 years, were investigated. The objective was to identify any differences in urinary metabolites according to sex and age (Liu et al., 2022). In a separate study, the urinary metabolites of children with an autism spectrum disorder were examined to investigate the potential correlation between the disease and an altered gut microbiome (Srikantha and Mohajeri, 2019).

1.8 NMR-Spectroscopy

Nuclear magnetic resonance is a spectroscopic technique based on the reorientation of atomic nuclei in an external magnetic field. This requires an atomic nucleus with non-zero nuclear spins, such as 1H, 13C, or 31P. Depending on the isotopic composition of the nucleus, this reorientation occurs when electromagnetic radiation, commonly in the radiofrequency range of 4 to 900 MHz, is absorbed. It is enhanced in direct proportion to the strength of the external magnetic field (Slichter, 1963, Friebolin, 2013).

In order to perform these measurements, at first a constant magnetic field has to be applied on the sample to polarize the nuclear spins. The next step is the perturbation of the nuclear spins by a weak oscillating magnetic field, followed by the detection of the electromagnetic waves emitted by the nuclei of the sample. As the responded signal is highly representative for the electrical environment of the nuclei, the signal can be assigned to specific molecules or substances with high accuracy, as long as the signal outputs are known in advance (Slichter, 1963). Furthermore, the concentration can be determined via H1-NMR spectroscopy, as the integral of the respective signals is directly contributed with the number of the specific hydrogen nuclei and therefore the concentration. However, since the concentrations in urine are highly dependent on the amount of fluid consumed, the relative proportion to the creatin concentration is given instead (Bouatra et al., 2013, Budde et al., 2016).

Consequently, high-resolution NMR spectroscopy is ideal to analyze the complex composition of urine and estimate the quantification of urinary metabolites. As urine is an aqueous solution, the proton signal of water has to be suppressed, which can be performed by using a f1 pre-saturation. Furthermore, a deuterated buffer solution must be used to suppress the signal of the included proteins. This finally leads to a specific detection of all non-exchangeable protons of small molecules by using typically frequencies of 500 or 600 MHz (Bouatra et al., 2013, Stryeck et al., 2018). Due to the received spectra, the contained substances of the sample and the relative contribution of these can be determined in a highly specific manner. According to Bouatra and colleagues unique urine metabolites or metabolite species could be detected and quantified by high-resolution NMR spectroscopy (Bouatra et al., 2013).

2. Aims and Objectives

As previously stated, the rise in the prevalence of overweight and obese children represents a significant public health concern. The range of secondary diseases is extensive, encompassing cardiovascular, orthopedic, dental, and mental health conditions. The causes of the increase in childhood obesity are also difficult to ascertain. The increased consumption of unhealthy foods and lack of exercise are significant contributing factors in this regard. Despite the efforts of numerous research groups, the issue of childhood obesity remains unresolved, with significant potential for further improvement.

This thesis focuses on the potential effects of childhood obesity on urinary metabolites. The objective was to ascertain which urinary metabolites are present in elementary school children and to derive conclusions regarding the pathological effects of obesity based on observed differences in the urinary metabolite profile of the individual groups classified by SAT. In consideration of the aforementioned evidence, it is proposed that:

1. The composition of metabolites in the urine of elementary school children differs significantly depending on the thickness of subcutaneous fat.
2. With regard to the thickness of subcutaneous fat, differences can be observed between girls and boys of elementary school age.

The data necessary for the completion of this study were gathered as part of the larger Happy Children study. For further details regarding the Happy Children study, please refer to (Goswami et al., 2022).

The prevalence of childhood obesity continues to rise at an alarming rate. It is of paramount importance that greater attention be devoted to the implementation of comprehensive health programs, coupled with augmented research initiatives and heightened awareness of the prevalence of childhood obesity. In the future, the identification of obesity may be accomplished via a non-invasive urine test, which could facilitate early diagnosis.

3. Methods

3.1 Study design

This thesis was conducted as part of the Health and Academic Performance with Happy Children (HAPHC), short 'Happy Children'–study, a project which aimed at improving health and academic performance in elementary school children by implementation of a daily session of physical activity across the curriculum (PACC). For the HAPHC-study 12 elementary schools from three different European countries (Austria, Slovenia, Belgium) were recruited to act as either an intervention or as control school in a large intervention study. Based on the Norwegian Health Oriented Pedagogical Project (HOPP) study (Fredriksen et al., 2017), the teachers at the intervention schools received training and teaching equipment that allowed them to integrate a daily physical activity sessions of 45 minutes across the curriculum. Additionally, teachers were asked to record the number of PACC lessons they managed to perform weekly. The teachers were asked to redesign the instructional approach and learning materials during the implementation of active learning to optimize them with reference to their local curricula and other specific requirements. The aim of the study was to find out how the daily physical activity changes health related physiological factors, academic achievement, psycho–social aspects and wellbeing. (for details please refer to (Goswami et al., 2022).

The present thesis investigated the relation between the amount of subcutaneous adipose tissue measured by B-mode (brightness-mode) ultrasound and the composition of urine in children aged 6 to 11 years. The data were collected from children of the three participating elementary schools in Graz, Austria. The data analyzed within the present thesis were conducted from the baseline measurements, raised in autumn of 2021, before the start of the intervention. After collection of the baseline data, two schools were allocated to the intervention group, one acted as the control school. In total, 473 children were enrolled in the study and investigated for study purposes.

3.2 Ethical approval

The study was approved by the local Ethics Committee of the Medical University of Graz, Austria (33-488 ex 20/21), and is registered in the ClinicalTrials.gov (NCT04956003). Participation in the HAPHC project was voluntary, and the signed consent from parents or legal representatives was a requirement for participation. All children of the intervention

schools took part in the intervention, though only children with written consent of their parents/legal representatives were measured and tested for study purposes(Goswami et al., 2022). Each child was also given the opportunity to refuse an individual measurement or withdraw the entire testing at any time.

3.3 Recruitment

End of February 2021, an invitation letter for participation in the Health and Academic Performance with Happy Children program was send out by the Board Directorate of Education Styria to all 42 public elementary schools in Graz. Two voluntarily participating schools were each assigned to act as intervention school, one school acted as a control school. A total of 353 children aged 6-11 years (grades 1, 2, 3, and 4) were included in the study, which involved the measurement of subcutaneous adipose tissue SAT and the administration of urinary metabolite tests (Figure 5).

Children of different socioeconomic backgrounds, cultural contexts and both sexes took part in the measurements. No child was excluded a priori. However, any pre-existing disability or illness was recorded and considered when validating the results of the children. Moreover, each child had the opportunity to deny participation at any time of the study or for a certain measurement. The number of cases was chosen, based on a sample size estimation and results of a comparable study carried out in Norway (Health Oriented pedagogical project,(Fredriksen et al., 2017)) (Goswami et al., 2022).

For the present thesis, the baseline data of children from all three schools were pooled together. Based on the amount of their SAT as assessed by B-mode ultrasound (see section 3.5.1. SAT-Measurement), the children were divided into tertials and the profile of the urine metabolomics of each group was compared with each other.

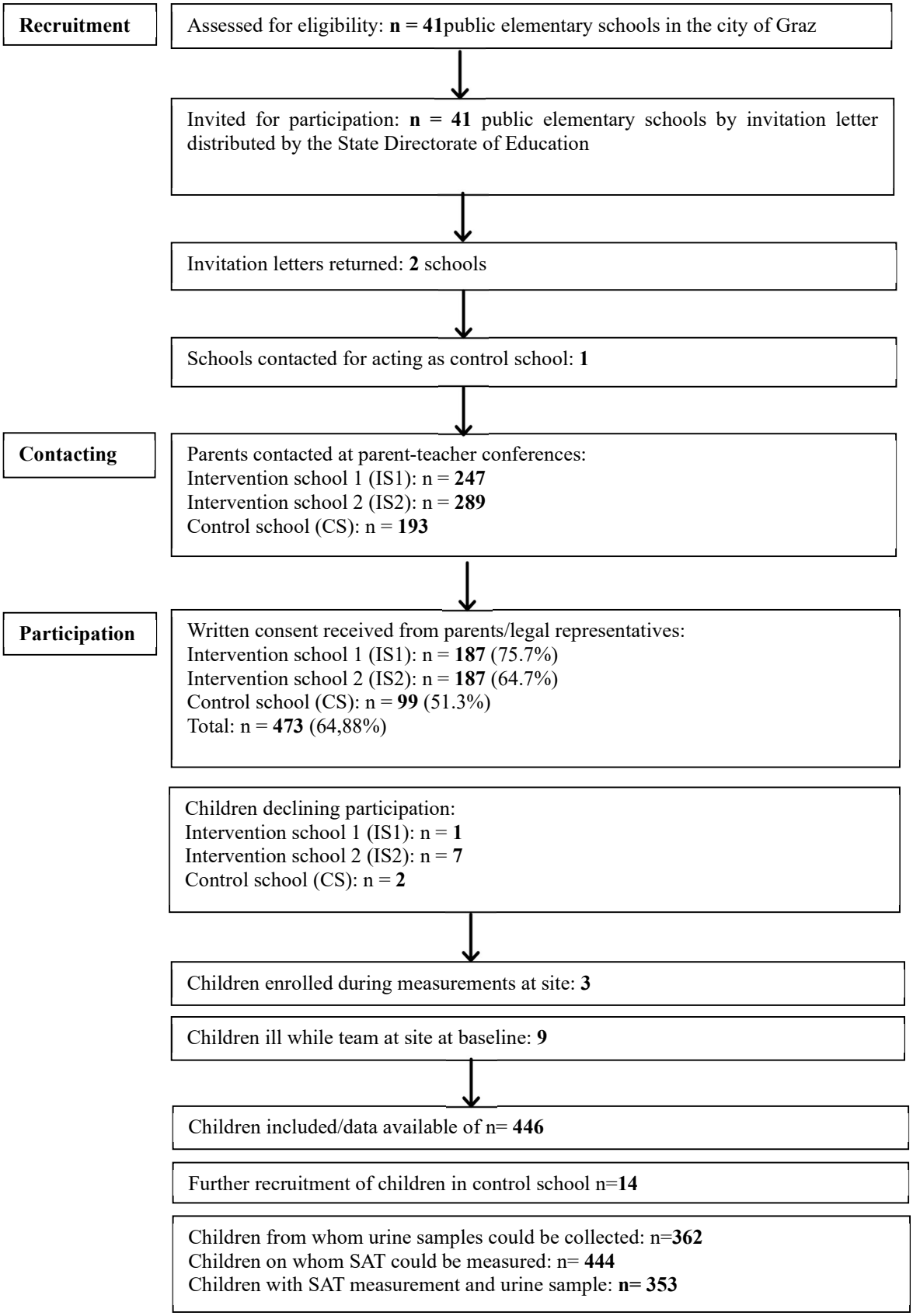

Figure 5: Recruitment process of the study participants: n= number of children

3.4 Protocol and setting

Baseline measurements were taken in September 2021, before the start of the intervention. The follow-up measurements were taken; at the end of each school year starting in June 2022 (1st follow-up), June 2023 (2nd follow-up) and June 2024 (3rd follow-up).

In addition to the measurement of subcutaneous adipose tissue and collection of urine samples, several other tests were performed to assess physical fitness, cognitive performance, and other medical parameters, but these are not part of the present study. All tests and examinations performed within the HAPHC study were non-invasive and standardized. For details please refer to (Goswami et al., 2022).

Measurements were conducted in the gymnasiums and locker rooms of each school in small groups of 4-6 children and performed between 8 am and 2 pm. Urine samples were collected in the morning, cooled at -80°C and examined after a period of approximately 4 months using NMR spectroscopy.

At no time was a child left alone in a room with only one examiner. Efforts were also made to ensure that children were examined by examiners of the same sex. The collected measurements, especially the weight, were not communicated to the children or in front of other children.

3.5 Measurements

3.5.1. SAT-Measurement

The Subcutaneous Adipose Tissue (SAT) was measured with a B-mode (brightness mode) ultrasound system (Esaote laptop color Doppler system, SMT, Germany). Ultrasound uses the pulse-echo technique for the construction of its images. An applied ultrasound pulse travels with a certain speed in a given tissue. The majority of diagnostic ultrasound machines use a speed of 1540 m/s. At 2-dimensional imaging, ultrasound beams get sent into the tissue for creating an image in which the brightness of the screen (B-mode) corresponds to the echo intensity in the plane of the scan.

The spatial resolution is limited by diffraction, which is proportional to the wavelength that is in use. Frequencies between 10-22 MHz are typically used for soft tissues of 0.5-0.07 mm.

The accuracy of ultrasound fat-thickness measurement was found to be excellent (Müller et al., 2020). The technical error in intra- and interobserver studies was less than 0.6mm at all sites investigated. Using ultrasound, the subcutaneous adipose tissue is easy to locate because it forms a continuous layer under the skin and is bordered by the muscle fascia below. For a good accuracy of this technique, the investigator has to visually control the output of automatic edge detection algorithms to prevent inaccurate image interpretations (Schmid-Zalaudek et al., 2021, Müller et al., 2020).

Anthropometric data has to be collected to estimate total subcutaneous fat. Anthropometric measurements include body height (h), sitting height (s), leg length (l), body mass (m) and the circumferences of the waist (W), hip (H), biceps (B) and thigh (T). Height was measured using a stadiometer while standing and without shoes. This allowed the height to be recorded with an accuracy of up to 0.1cm. Body weight was measured using an electronic scale (Tanita MC-980MA, Tokyo, Japan) while wearing shorts, a T-shirt, and no socks. Body weight was measured with an accuracy of up to 0.1kg. To obtain the actual body weight, 0,4 kg was subtracted from the recorded measurements for clothing worn. The waist circumference, hip circumference, biceps, thigh, leg length and the sitting height were measured with a tape measure with an accuracy of 0.1cm. The waist circumference was measured at the narrowest point of the waist in mid-breath position, while the hip circumference was measured at the biggest point of the bum. The biceps was measured at the thickest point while flexed and the thigh circumference was measured at the US-measurement point frontal thigh (see Table 1 and Figure 6 below). The sitting height was measured in an upright position, sitting on a table, with the feet placed on a box. To determine the leg length, the distance from the floor to the spina iliaca anterior superior was measured while standing.

Eight measurement points were marked for subcutaneous adipose tissue determination. To obtain the most accurate results, it is important to accurately locate the measurement points on the body. Table 1 describes how to determine the measurement points in detail (Müller et al., 2016).

Table 1: Description of ultrasound sites and measurement procedure (Müller et al., 2016)

Site name	**Description of the sites** **Marking is done in a standing or sitting position, on the right side of the body; see Figure 6. All distances (d) are percentages of body height (h)**	**All US measurements are taken in a lying position!** **Always use a thick layer of US gel (at least 3–5 mm)**
UA **Upper abdomen**	1. Mark a vertical line at a distance d=0.02 h (2% of body height h) lateral to the center of the umbilicus (omphalion) 2. Project vertically and mark a horizontal line at d=0.02 h superior to the omphalion (Figure 6A). (In case this site is above a tendinous inscription of the rectus abdominis (where subcutaneous adipose tissue (SAT) is thicker), move the probe some mm to the end of this inscription and measure the thickness there)	Lying in a supine position. Have the participant stop breathing at mid-tidal expiration and then capture the image
LA **Lower abdomen**	1. The same line as for the upper abdomen 2. Project vertically and mark a horizontal line at d=0.02 h inferior to the omphalion (Figure 6A).	Lying in a supine position. Have the participant stop breathing at mid-tidal expiration and then capture the image.
FT **Front thigh**	1. Put the foot on the anthropometric box which is placed in front of a wall so that the thigh is horizontal and the big toe and the knee touch the wall. 2. Mark the site at a horizontal distance d=0.14 h from the wall (Figure 6E).	Lying in a supine position.
LT **Lateral thigh**	1. Place the foot on the anthropometric box so that the thigh is horizontal and the leg is vertical. 2. Mark the site at d=0.18 h above the surface at the most medial aspect (use a ruler to determine the most medial aspect when looking vertically down (Figure 6F).	Lying in a rotated position. The participant rolls onto the left side with both knees at a 90° angle, with the right leg over the left leg.
MC **Medial calf**	1. Place the foot on the anthropometric box so that the thigh is horizontal and the leg vertical 2. Mark the site at d=0.18 h above the surface at the most medial aspect (use a ruler to determine the most medial aspect when looking vertically down Figure 6F).	Lying in a rotated position. The participant rolls onto the right side with the right knee at a 90° angle so that the lateral aspect of the right leg is supported.
ES **Erector Spinae**	1. Mark a transverse line at d=0.14 h above the solid surface (table) on which the person is sitting in a stretched upper body position with thighs horizontal and legs unsupported. 2. Mark the site at d=0.02 h lateral to the spinous process of the vertebra (Figure 6C).	Lying in a prone position.

DT **Distal Triceps**	1. Put the lower arm on a support surface (table) with the hand in the mid-prone position. Mark a vertical line on the most posterior aspect of the arm. 2. Mark the site on the vertical line at a distance from the surface of d=0.05 h (Figure 6D).	Lying in a prone position. Capture the image with the dorsal surface of the hand on the table. Make sure the probe orientation is perpendicular to the skin.
BR **Brachioradialis**	1. The participant puts the forearm with the hand in the mid-prone ('shake-hands') position on a support table and contracts the brachioradialis (Figure 6D). 2. Draw a longitudinal line on the most anterior surface of the brachioradialis muscle. 3. Mark a transverse line at a distance d=0.02 h distally from the anterior surface of the biceps brachii tendon (press the end of the metre rod onto the stretched tendon). Project this line transversely to intersect with the longitudinal line (Figure 6D).	Lying in a supine position. Take the image with the arm in a mid-prone position and in contact with the thigh (muscles of the arm are relaxed). Avoid imaging the vein in case there is one in the vicinity.

In order to provide an overview of the measurement points described in Table 1, they are shown on a test subject in Figure 6.

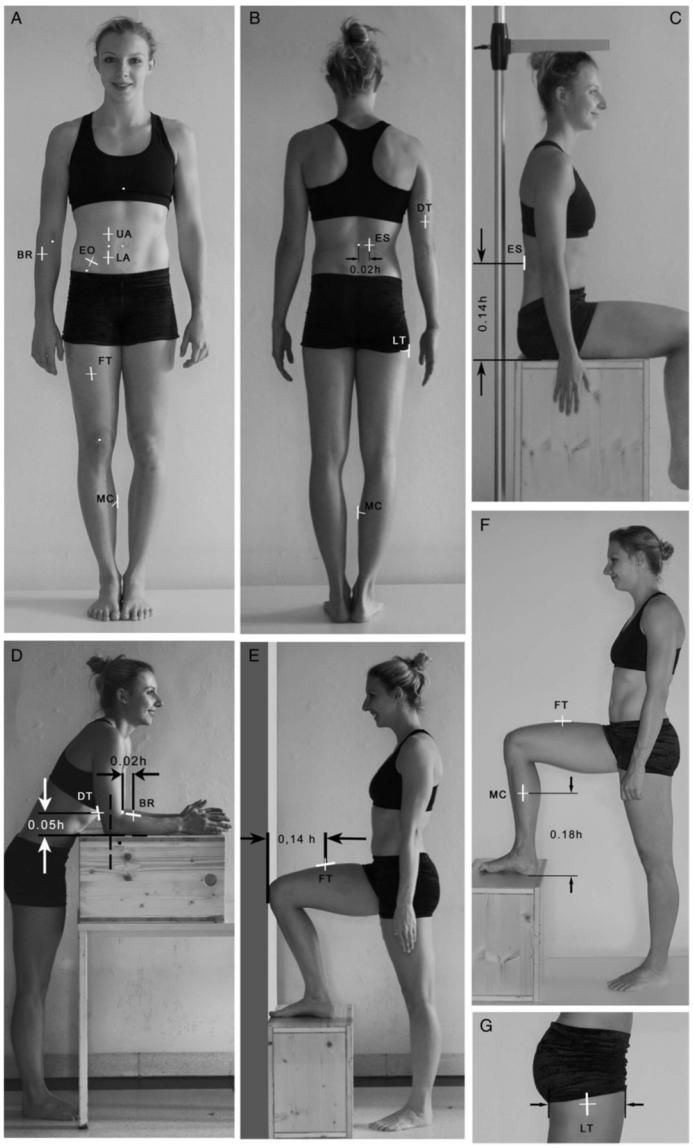

Figure 6: Ultrasound sites: Note, that the site EO (external oblique) was replaced by the lateral thigh because it caused measurement problems in obese individuals and had a worse reliability. Furthermore, the lateral thigh site is a typical location for fat depots in women (Müller et al., 2016).

In all ultrasound images, the same sequence of layers can be seen at all measurement points. Figure 7 shows a typical ultrasound image of the subcutaneous adipose tissue. To make sure where the muscle fascia is located, the layers can be compressed. Fat is more easily compressed than muscle tissue and so the muscle fascia can be precisely determined (Müller et al., 2016).

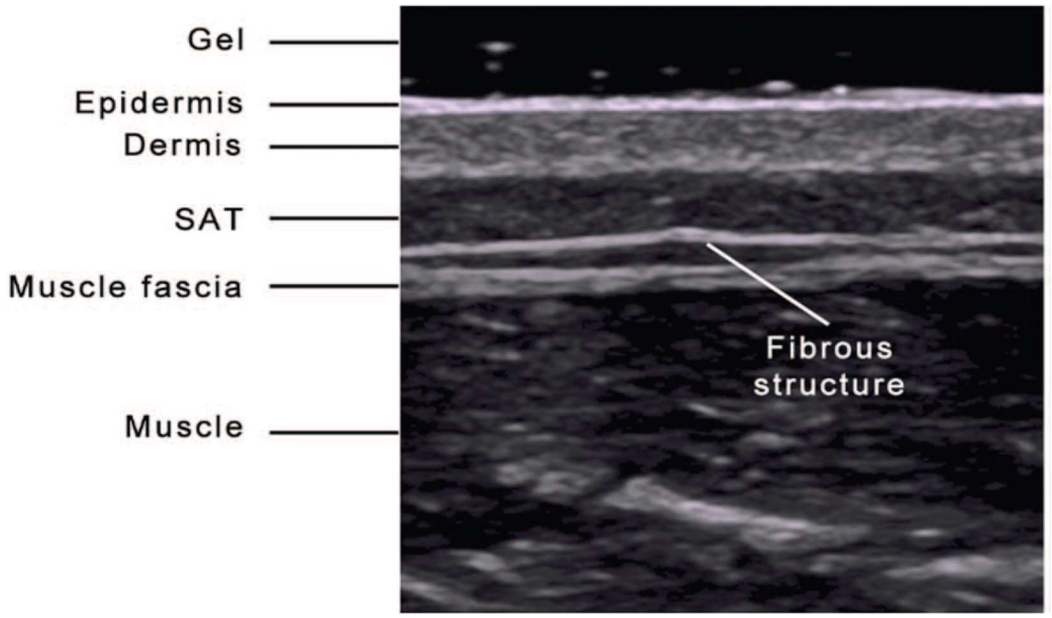

Figure 7: A typical ultrasound image of the subcutaneous fat (Müller et al., 2016)

To detect the contour of the subcutaneous fat on the individual images an interactive image segmentation was applied and the software (NISOS-BCA-F4.2; rotosport.at) automatically performed thickness measurements for each ultrasound picture of all eight sites. Reliability studies have shown that the limit of agreement for the sums of the eight thickness measurements is between 1 and 2 mm (Schmid-Zalaudek et al., 2021, Müller et al., 2020, Kelso et al., 2020, Störchle et al., 2017).

For the present study, the sum of the subcutaneous adipose tissues from all eight measurement points, including the fibrous structures embedded in the fat, was taken to determine the obesity in the children. This value was used to categorize the groups in terms of subcutaneous fat, as it is a measured value with no additional assumptions or calculations. The fasciae within the fat are included in the measurements because it has been shown that even minimal tilting of the ultrasound probe can cause variations in the amount of fibrous structures in the ultrasound image. Therefore, the thickness of the subcutaneous fat including the fascia within the fat (D_I) was used.

3.5.2 NMR-Spectroscopy

A common and highly selective method for the quantification and identification of urinary metabolites is the high-resolution Nuclear magnetic resonance spectrum (Bouatra et al., 2013). NMR-spectroscopy was conducted as part of this study, following the methodology outlined below:

After thawing, 60 µl of IVDr sample buffer were mixed with 540 µl of urine for each sample into 5 mm/4 inch NMR glass tubes. After mixing, samples where directly measured (in patches of 96 samples) at 300 K using a 600 MHz Bruker Avance Neo NMR spectrometer (Bruker Biospin, Rheinstetten, Germany) equipped with a TXI 600 probe head. NOESY (noesygppr1d, NS = 32, TD = 65536, SI = 131072) and 2D-JRES (jresgpprqf, NS = 2, TD = 8192/40, and SI = 16384/256 for F2/F1, respectively) spectra were recorded for each sample according to the manufacture's instructions. For quantification of up to 150 metabolites within one urine sample a special server-based algorithm called B.I.Quant-UR ne^{TM} (Bruker) was used to extract relevant information from sample spectra. As a final output, an Excel sheet with all samples and all metabolites got prepared, both with free concentrations (in mmol/L) and, more relevant in urine due to varying fluid uptake, concentrations normalized on creatinine (mmol/mol CREA).

3.6 Statistical analysis

Explorative data analysis was performed on all raw data to check for potential outliers (± 3SD), valid or implausible scores, with the latter being removed or excluded from further analyses. Children were classified and assigned to one of three groups by their total sum of SAT (including fibres D_I) according to the cut-off values for terciles p=1/3 and p=2/3, resulting in three almost equal numbered groups T1, T2, T3 (T1 (least subcutaneous fat), T2 (second-most subcutaneous fat), and T3 (most subcutaneous fat)).

Univariate analysis (like volcano plots) and multivariate analysis like principal component analyses (PCA), and more importantly, orthogonal partial least squares discriminant analysis (oPLS-DA) were performed to extract the most relevant markers using the freely availably server-hosted statistical software Metaboanalyst (https://www.metaboanalyst.ca/) (Pang et al., 2024). Further analyses were done using the statistical software Rstudio/R (v 4.3), using packages rstatix (for multiple ANOVA) and co-occur (for co-occurrence analysis), amongst others.

Descriptive statistics were calculated by IBM SPSS (Statistics for Windows, Version 28.0. Armonk, NY: IBM Corp). To prevent alpha-inflation, p-values, usually considered as significant at a level of $p<.05$, false discovery rate (FDR) was applied for correction.

4. Results

In total, 460 of 471 children of whom written consent was obtained by their parents, were enrolled in the baseline measurements (due to absence at time of data acquisition or withdrawal from the study). SAT was measured in 444 children (96.5%; 216 = 48.6% of them girls) and urine samples were collected in a total of 362 children. The missing SAT scores and urine samples were due to refusals by the children.

For the research question of the present thesis, data of 353 children with both, urine samples and SAT measurement, were included for comparisons of tercile-based groups (T1, T2 and T3). The first group was defined by a cutoff value of $D_I \leq 46.61$ mm, while the second group was defined by a cutoff value of $D_I \leq 77.56$ mm. The first group comprised 118 children, the second 117, and the third 118.

4.1 Participants

The sample (n=353) included children aged 6 to 11 years. No significant differences were found in the number of girls and boys ($\chi 2_{(df=2)} = 0.327$, p=.849). In all three schools a similar number of boys (52.4%) and girls (47.6%) provided their urine sample and took part in the SAT measurements. Only with regard to height, boys were found to be significantly taller than girls ($t_{(351)}$=-2.378, p=.018) (see Table 2).

Table 2: Characteristics of participants

	Sex	n	Mean	SD	Min.	Max.
Age [years]	Girls	168	7.78	1.32	6.00	11.00
	Boys	185	7.95	1.28	6.00	11.00
Height [m]	Girls	168	1.32	0.10	1.12	1.58
	Boys	185	1.34	0.09	1.14	1.57
Weight [kg]	Girls	168	31.40	10.60	17.80	73.10
	Boys	185	32.17	8.85	19.90	71.60
BMI [kg/m^2]	Girls	168	17.62	3.67	12.04	31.55
	Boys	185	17.55	3.16	13.31	31.02
WHtR	Girls	168	0.45	0.05	0.33	0.65
	Boys	185	0.45	0.05	0.33	0.68

Abbreviations: n = number of children, SD = standard deviation, Min = Minimum, Max = Maximum, BMI = body mass index, WHtR = waist to height ratio

4.2 Subcutaneous adipose tissue (SAT)

The total amount of the SAT as measured at the eight standardized sites (sum mean included) of each individual was split into terciles, applying cut of scores for 1/3 (D_I= 46.61) and 2/3 (D_I= 77.63), resulting in almost equal sized groups. Subcutaneous fat was assessed in 347 children, with measurements taken at eight points.

Four children exhibited a lack of data regarding the measurements of the site brachioradialis. In this instance, a seven-point measurement was conducted, encompassing the upper abdomen, lower abdomen, front thigh, lateral thigh, medial calf, erector spinae and distal triceps. The evaluation program subsequently calculated the missing value using the anthropometric data. For two children, only the measurements of the upper abdomen, lower abdomen, front thigh, and lateral thigh were available. In this case, these four sites were utilized to determine the subcutaneous fat, while the remaining four sites were calculated as previously described.

Notably, the number of children assigned to the three groups differed significantly between the schools (χ^2_4= 42.98, p<.001). A larger number of children assigned to group T3 (high amount of SAT) was found in IS-1 (47.1%) and the CS (41.4%) while in IS-2 only 14.1% of the children were assigned to the third tercile. Table 3 shows the assignment of children to the terciles according to their total sum of SAT (D_I) by school. Figure 8 illustrates the notable discrepancy in the thickness of the subcutaneous fat on the abdomen of two children of comparable height.

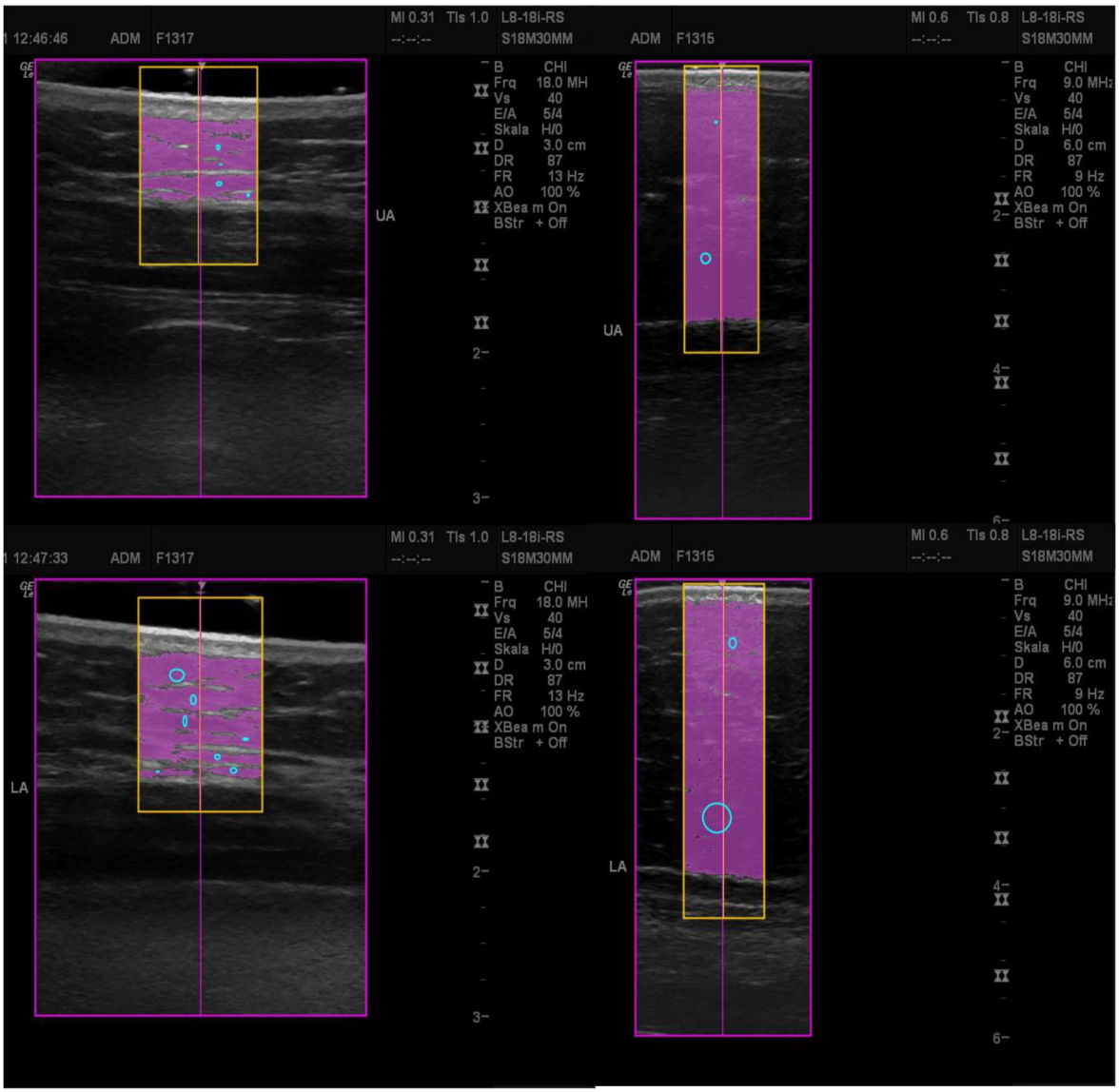

Figure 8:Ultrasound pictures of different amounts of SAT. The images on the left demonstrate the ultrasound measurements of the abdominal walls of a child with minimal subcutaneous adipose tissue, whereas the images on the right illustrate those of a child with a similar height but a greater amount of subcutaneous adipose tissue. It is important to note that the images on the right were obtained with a penetration depth of 6mm, which is twice that of the images on the left (3mm). The differences in thickness are therefore actually even more striking.

Table 3: Number of children assigned to the SAT terciles by school

SAT-group	Cut-off [mm]		School			Total
			CS	IS-1	IS-2	
T1	< 46.6	n	17	34	67	118
		% of school	26.2%	22.2%	49.6%	33.4%
T2	46.6 to 77.6	n	21	47	49	117
		% of school	32.3%	30.7%	36.3%	33.1%
T3	> 77.6	n	27	72	19	118
		% of school	41.5%	47.1%	14.1%	33.4%

Abbreviations: IS-1 = Intervention school 1, IS-2 = Intervention school 2, CS = Control school, n=number of children

In total, girls showed a higher amount of SAT ($D_{I\ girls}$ = 79.28 ± 42.28) as compared to boys ($D_{I\ boys}$ = 64.52 ± 40.58, $t_{(351)}$= 3.346, p<.001) and thus were more frequently assigned to T3 than boys (χ^2_2 = 18.36, p<.001, see Table 4).

Table 4: Frequency of girls and boys assigned to the SAT terciles

SAT-group	Cut-off [mm]		Sex		Total
			Girls	Boys	
T1	< 46.6	n	38	80	118
		% of sex	22.6%	43.2%	33.4%
T2	46.6 to 77.6	n	60	57	117
		% of sex	35.7%	30.8%	33.1%
T3	> 77.6	n	70	48	118
		% of sex	41.7%	25.9%	33.4%

Abbreviations: n = number of children

The total sum of SAT (including fibres) varied considerably between the samples ranging from a minimum of 10.09 mm up to a maximum of 208.77 mm with the upper and lower abdomen as well as the lateral thigh being the sites with highest amounts of SAT. Table 5 gives an overview of the SAT distribution at the eight measurement sites in the three (tercile-split) groups.

Table 5: Thickness of sites in the three SAT-groups

Site	SAT-group	n	Min.	Max.	Mean	SD
Upper Abdomen	SAT-T 1	118	0.44	5.38	1.98	0.98
	SAT-T 2	117	1.81	13.56	5.80	2.32
	SAT-T 3	118	6.79	43.45	20.02	8.79
Lower Abdomen	SAT-T 1	118	0.38	10.85	5.02	2.35
	SAT-T 2	117	4.32	20.03	11.15	3.36
	SAT-T 3	118	13.09	55.15	27.44	8.79
Front Thigh	SAT-T 1	118	1.13	8.21	5.04	1.33
	SAT-T 2	117	5.00	12.48	7.98	1.39
	SAT-T 3	118	6.81	25.15	13.41	3.58
Lateral Thigh	SAT-T 1	118	1.44	14.80	7.78	2.78
	SAT-T 2	117	6.65	24.73	13.69	2.96
	SAT-T 3	118	11.93	42.19	22.91	6.19
Medial Calf	SAT-T 1	118	1.20	5.98	3.43	0.98
	SAT-T 2	116	2.84	14.38	5.29	1.50
	SAT-T 3	117	3.82	18.78	9.24	2.84
Erector Spinae	SAT-T 1	118	0.52	5.67	2.17	0.93
	SAT-T 2	116	1.46	9.03	4.46	1.43
	SAT-T 3	117	2.87	24.36	9.68	3.92
Distal Tricesp	SAT-T 1	118	0.91	8.71	5.55	1.40
	SAT-T 2	116	3.37	10.77	7.72	1.44
	SAT-T 3	117	4.45	22.86	12.12	3.54
Brachioradialis	SAT-T 1	117	0.64	5.62	2.74	0.84
	SAT-T 2	115	2.18	12.48	4.17	1.08
	SAT-T 3	115	3.22	11.27	6.36	1.58
Total	SAT-T 1	118	10.09	46.61	33.73	8.53
	SAT-T 2	117	46.78	77.33	60.05	9.04
	SAT-T 3	118	77.63	208.77	120.76	33.68

Abbreviations: n = number of children, Min = Minimum, Max = Maximum, SD = Standard Deviation

4.3 Occurrence of Metabolites in urine in the total sample (n= 362)

The variance of metabolite occurrences in urine was high. Creatinine (as expected) was found in every sample, other metabolites, e.g. alanine, dimethylamine (DMA), citrate, glycine, hippurate, and many other metabolites were measured in more than 10% of all samples (see Figure 9**Fehler! Verweisquelle konnte nicht gefunden werden.** and Table 6). Included are highly abundant amino acids, end products of metabolism (e.g. DMA, hippurate), and e.g. ketone bodies (acetoacetate).

Interestingly, glucose was measured in 22% (79 of 362 cases) of the whole sample. Since glucose in urine might be a preliminary indicator of diabetes, this number seems fairly high. The cut-off value of the applied NMR method (limit of detection, LOD) is 0.67 mM, ending up with 22% of total samples. In view of a reference value (for adults though) for glucose in urine of < 0.83 mM (Gressner, 2013), only 23 samples (6.4%) may be regarded as "glucose-positive". Still, this is quite a high number in face of the children's age.

Low abundant metabolites (occurrence < 10%) again include some amino acids (e.g. leucine), sugars (e.g. galactose), and many acids (e.g. 4-amino-butyrate, fumarate, 2-hydroxyphenylacetate, lactate etc.), see Table 7. Many metabolites, which could be detected in principal, could not be measured in any sample.

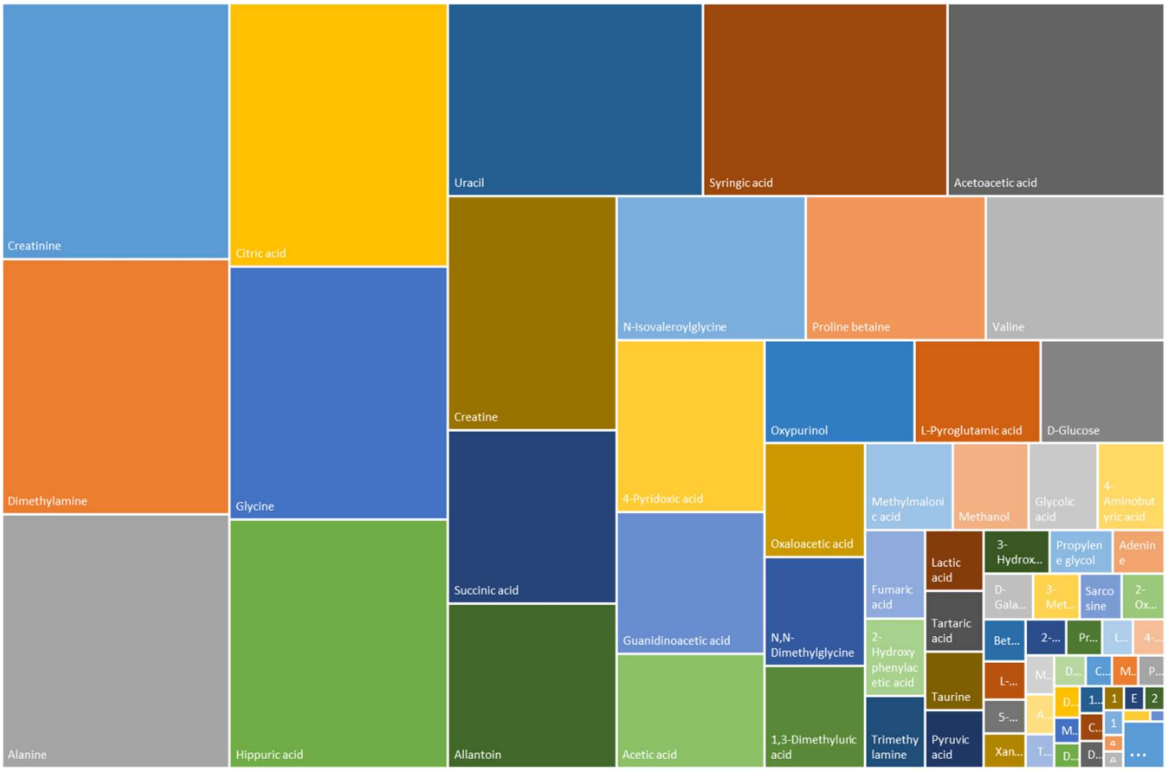

Figure 9: Metabolome of the whole cohortdisplayed as relative occurrence of measured analytes. Some metabolites dominate the spectrum as for instance (occurrence of creatinine = 1)

Table 6: Highly abundant metabolites (occurrence > 10%)

Metabolite	Occurrence	Metabolite	Occurrence
Creatinine	1 000	Proline betaine	0.445
Dimethylamine	0.997	Valine	0.439
Alanine	0.992	4-Pyridoxic acid	0.436
Citric acid	0.986	Guanidinoacetic acid	0.359
Glycine	0.945	Acetic acid	0.290
Hippuric acid	0.931	Oxypurinol	0.265
Uracil	0.845	L-Pyroglutamic acid	0.224
Syringic acid	0.809	D-Glucose	0.218
Acetoacetic acid	0.718	Oxaloacetic acid	0.196
Creatine	0.674	N,N-Dimethylglycine	0.188
Succinic acid	0.500	1,3-Dimethyluric acid	0.177
Allantoin	0.475	Methylmalonic acid	0.130
N-Isovaleroylglycine	0.467	Methanol	0.113
		Glycolic acid	0.102

Many metabolites (n=56) occurred only in a few samples (< 10%) (Table 7), while 67 metabolites were not detected at all.

Table 7: Metabolites of low occurrence (< 10%)

Metabolite	Occurrence	Metabolite	Occurrence
4-Aminobutyric acid	0.099	Maleic acid	0.014
Fumaric acid	0.091	Pantothenic acid	0.014
2-Hydroxyphenylacetic acid	0.080	D-Mannose	0.014
Trimethylamine	0.075	Methionine	0.011
Lactic acid	0.061	D-Mandelic acid	0.011
Tartaric acid	0.061	1-Methylhydantoin	0.011
Taurine	0.058	Cytosine	0.011
Pyruvic acid	0.058	D-Lactose	0.011
3-Hydroxyisovaleric acid	0.050	1-Methylguanidine	0.008
Propylene glycol	0.047	Ethylmalonic acid	0.008
Adenine	0.039	2-Hydroxyisovaleric acid	0.008
D-Galactose	0.039	1-Methylnicotinamide	0.008
3-Methylglutaconic acid	0.036	4-Ethylphenol	0.006
Sarcosine	0.033	Acetone	0.006
2-Oxoisovaleric acid	0.033	Caffeine	0.006
Betaine	0.030	Isopropanol	0.003
L-Threonic acid	0.028	DL-Tyrosine	0.003
5-Aminolevulinic acid	0.025	Benzoic acid	0.003
Xanthurenic acid	0.025	Phenylpyruvic acid	0.003
2-Oxoisocaproic acid	0.025	Trigonelline	0.003
Propionylglycine	0.022	L-Ascorbic acid	0.003
Leucine	0.019	2-Methylsuccinic acid	0.003
4-Hydroxyphenylacetic acid	0.019	3-Hydroxypropionic acid	0.003
Malic acid	0.019	D-Gluconic acid	0.003
Allopurinol	0.019	2-Oxoglutaric acid	0.003
Theobromine	0.017	4-Hydroxyphenylpyruvic acid	0.003
D-Mannitol	0.017	Orotic acid	0.003
Cystine	0.014	L-Fucose	0.003

Metabolites not detected at all (n=67): Ethanol, Tyramine, 1-Methylhistidine, 2-Furoylglycine, 3-Aminoisobutyric acid, 3-Methylcrotonylglycine, 5-Aminopentanoic acid, Arginine, Argininosuccinic acid, Citrulline, DL-Alloisoleucine, Glutamic acid, Glutamine, Isobutyrylglycine, L-Homocystine, L-Isoleucine, L-Tryptophan, N-Acetylaspartic acid, N-

Acetylglutamate, N-Acetylphenylalanine, N-Acetyltyrosine, Phenylalanine, Tiglylglycine, 3-Phenyllactic acid, 4-Aminohippuric acid, 4-Hydroxyhippuric acid, 4-Hydroxyphenyllactic acid, Phenylacetic acid, Pyrocatechol, E-Glutaconic acid, Formic acid, Glutaric acid, Imidazole, Propionic acid, Choline, D-Panthenol, Paracetamol, Paracetamol-glucuronide, 2-Hydroxy-4-methylvaleric acid, 3-Hydroxy-3-methylglutaric acid, 3-Hydroxyvaleric acid, Butyric acid, Citraconic acid, L-Citramalic acid, Pimelic acid, Thymol, 3-Hydroxyglutaric acid, D-Galactonic acid, 2-Ketobutyric acid, 3-Hydroxybutyric acid, 3-Methyl-2-oxovaleric acid, Acetoine, DL-Kynurenin, Succinylacetone, 1-Methyladenosine, Adenosine, Dihydrothymine, Dihydrouracil, Inosine, Neopterin, Quinolinic acid, Thymine, Uridine, D-Xylose, Galactitol, Glycerol, Myo-Inositol.

Next, we determined the co-occurrence of metabolites (Figure 10). It was calculated using the R package “cooccur” (Griffith et al., 2016).What it mainly does is to calculate, how often which metabolites occur within the same sample (“co-occurrence”) compared to arbitrary co-occurrence. Co-occurrence of metabolites, as calculated by the observed minus the expected co-occurrence of each pair of metabolites is shown in Figure 10. Those which co-occur more frequently, are closer together with each other.

For example, glycolic acid (occurrence 10.2%) is relatively often present, when, guanidinoacetate (3,8%), N,N-dimethylglycine (3,0%), 4-pyridoxic acid (2,7%), and lactate (2,2%), are also present in the respective sample. Additionally, succinic acid (occurrence 50,0%), which we found to be negatively associated with SAT (see below), revealed a high co-occurrence with acetic acid (6,5%), proline betaine (5,1%), acetoacetic acid (4,1%), methylmalonic acid (4,0%), methanol (3,1%), allantoin (3,0%), 4-aminobutyric acid (2,5%), and L-pyroglutamatic acid (2,1%). Allantoin (occurrence 47,5%) which is also negatively associated with SAT, was observed in conjunction with valine (4,3%), 4-pyidoxic acid (4,1%.), N-isovaleroglycine (3,8%), acetic acid (3,1%), succinic acid (3,0%), syringic acid (2,4%), and methanol (2,3%).

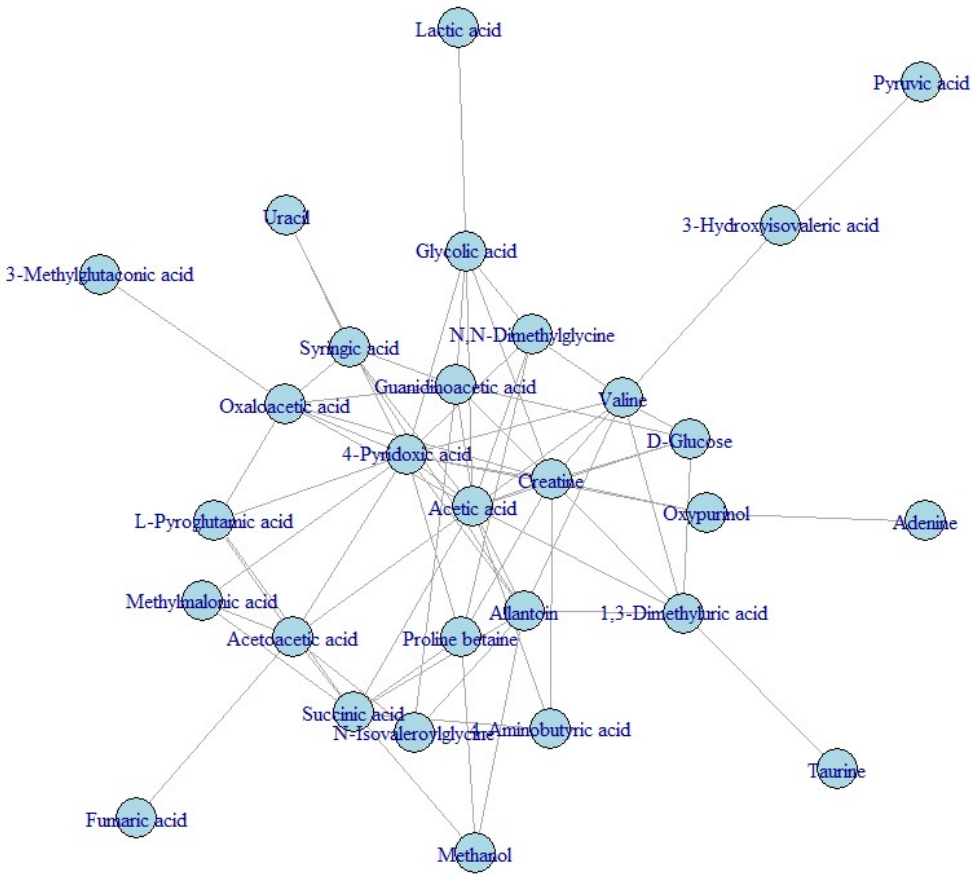

Figure 10: Co-occurrence of metabolites (only values >±0.02)

4.4 Sex differences

According to univariate ANOVA, parameters with highest and significant difference between males and females were acetic acid, D-glucose, succinic acid and adenine, which were throughout higher in girls (see Figure 11).

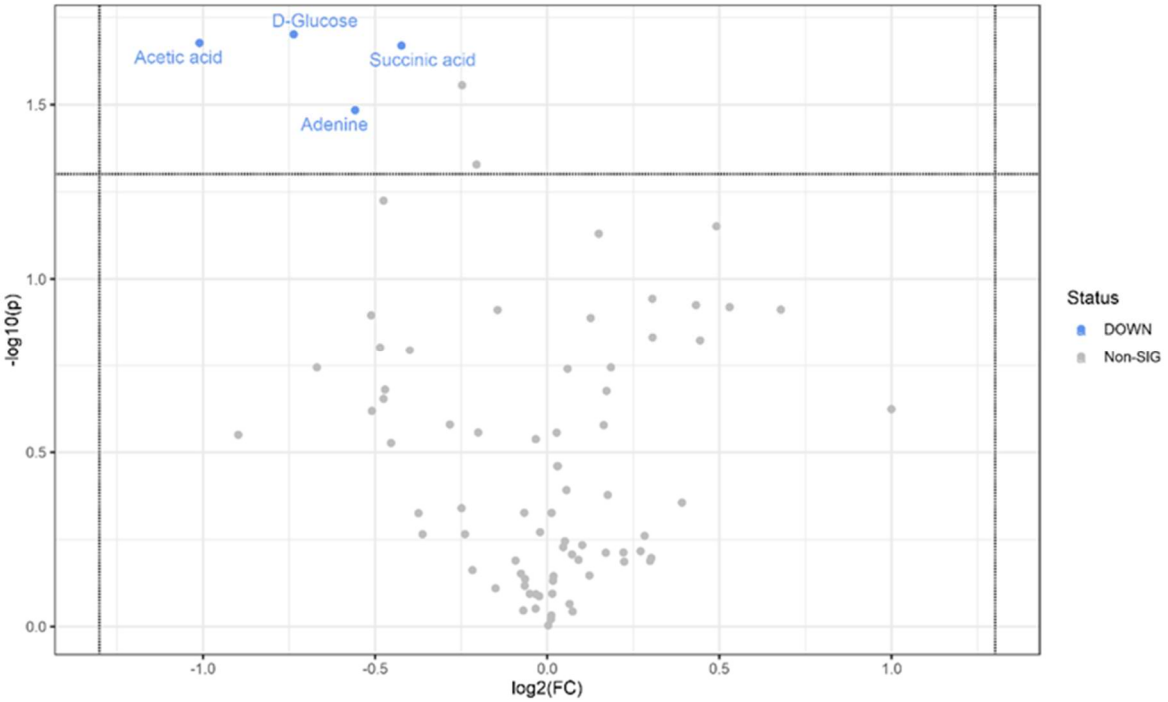

Figure 11: Sex differences in the occurrence of metabolites. Light blue indicates the metabolites which are higher in girls.

Orthogonal partial least squares discriminant analysis (oPLS-DA) revealed a significant difference between the sexes p(Q2 < 0.05), based on all (creatinine-normalized) metabolites (see Figure 12**Fehler! Verweisquelle konnte nicht gefunden werden.**).

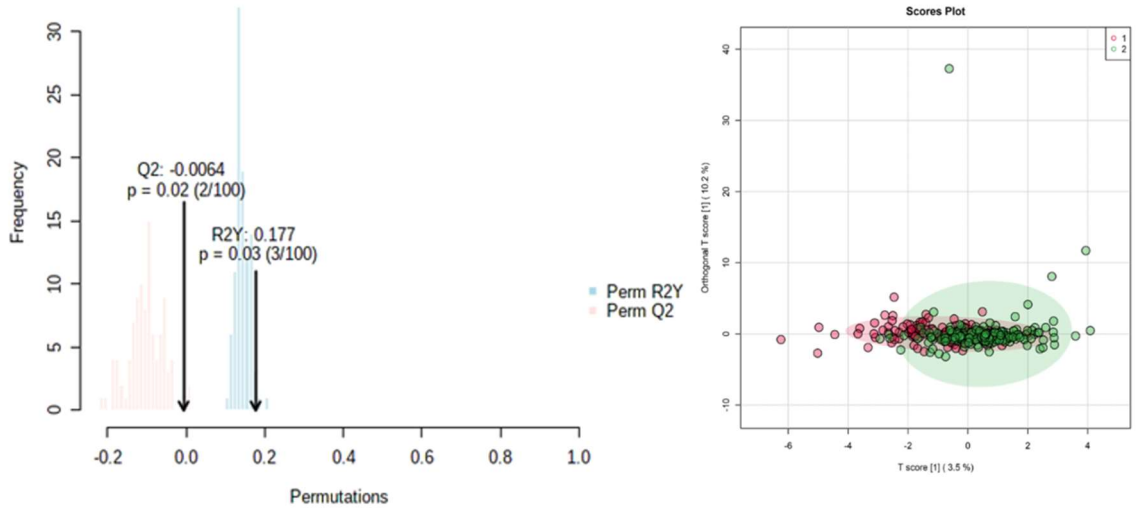

Figure 12: Sex differences made visible (oPLS-DA)

4.5 Height, weight and BMI

Succinic acid (r=-0.3135, p< .001, occurrence = 50%), dimethylamine (r=-0.2613, p< .001, occurrence = 48%) and allantoin (r=-0.2196, p< .001, occurrence = 47,5%) were the parameters showing highest association with weight as can be seen in Figure 13, and also with BMI (succinic acid: r=-0.251, p< .001, occurrence: 50%; dimethylamine: r=-0.158, p< .001, occurrence = 0.997; allantoin: r=-0.198, p=1.7E-04, occurrence: 0.475). Similarly, body height was also highly associated with these three metabolites, additionally to syringic acid (r=-0,206, p< .001, occurrence = 80,9%).

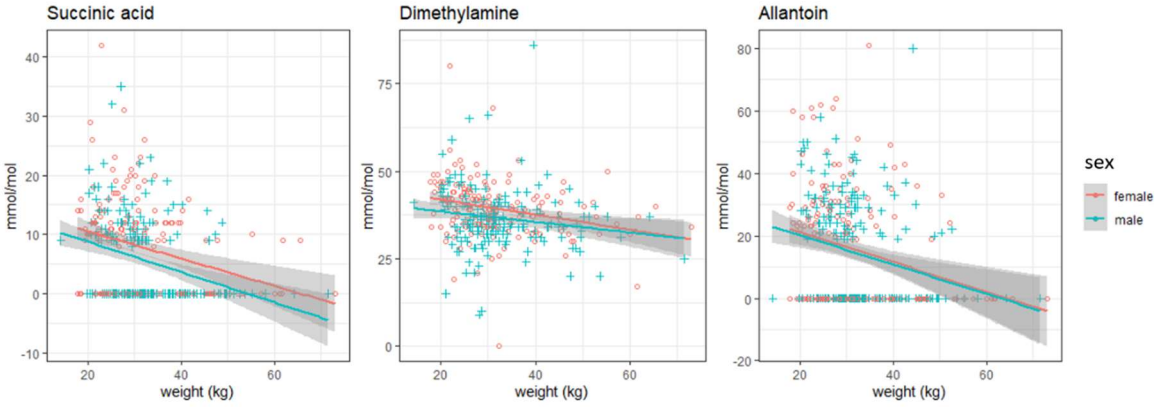

Figure 13: Association between concentration of metabolites and weight

4.6 Comparison of Metabolomics between the three SAT groups

For comparison of the three groups the creatinine normalized data were used and compared by one-way ANOVA, applying FDR for correction of p-values. The SAT tercile-based groups differed significantly with regard to allantoin ($F_{(1, 351)}$ =9.362, p=.002, $p_{corr.}$ = .034, Table 8, Figure 14) which was found to be highest in the group with fewer SAT (T1). This effect was, however, mainly based on the circumstance, that allantoin was found in a larger proportion of children (56.8%) with low SAT while in the high SAT group only in 36.4% of the children allantoin was found.

Table 8: Allantoin in the three SAT-groups

SAT-group	Mean	SD	n	cases
T1	18.90	18.55	118	67
T2	14.82	17.06	117	58
T3	11.84	17.59	118	43
Total	15.19	17.93	353	168

Abbreviations: n = number of children, SD = Standard Deviation, cases = children in whom allantoin was found

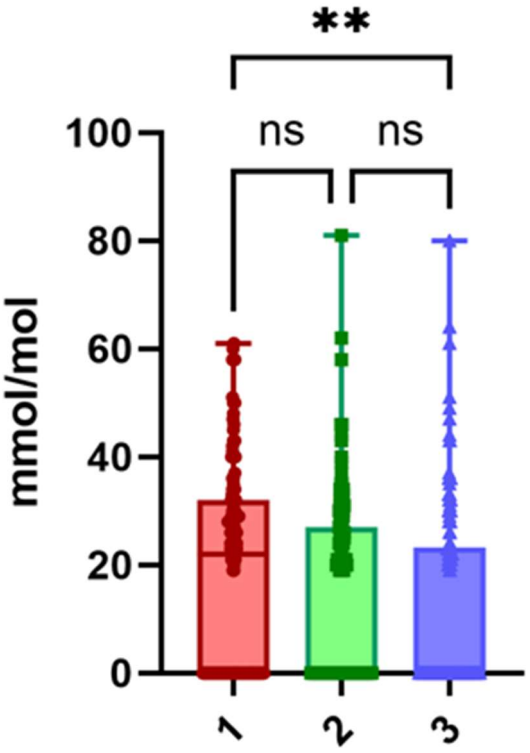

*Figure 14: Allantoin in the three SAT-groups: ns = not significant, ** = p<0.01, 1 = SAT-group T1, 2 = SAT-group T2, 3 = SAT-group T3*

Similar, for succinic acid a significant main effect was found ($F_{(1, 351)}$ =9.757, p=.002, $p_{corr.}$ = .034, Table 9, Figure 15), showing lowest concentration in children with high amount of SAT (T3). In only 38.1% of the children with high SAT and in 58.5% of the children with low SAT succinic acid was detected.

Table 9: Succinic acid in the three SAT-groups

SAT-group	Mean	SD	n	cases
T1	7.92	7.807	118	69
T2	7.54	8.182	117	63
T3	4.82	6.805	118	45
Total	6.76	7.721	353	177

Abbreviations: n = number of children, SD = Standard Deviation, cases = children in whom succinic acid was found

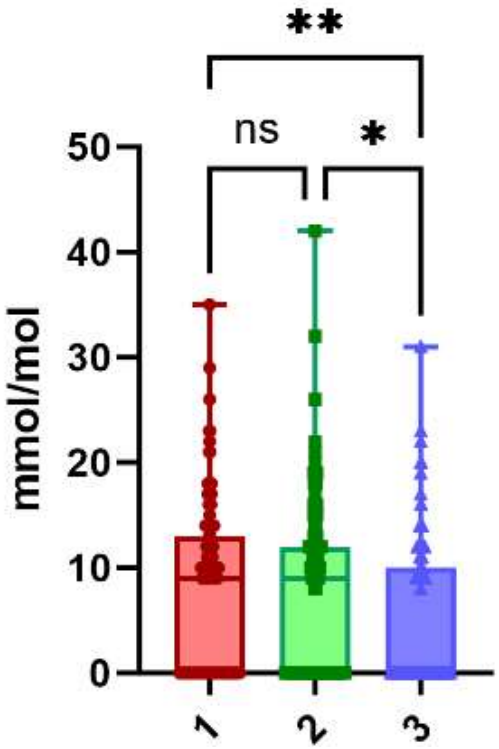

*Figure 15: Succinic acid in the three SAT-groups: ns = not significant, * = p<0.05, ** = p<0.01, 1 = SAT-group T1, 2 = SAT-group T2, 3 = SAT-group T3*

The differences observed for Glycine ($F_{(1, 351)}$ =4.836, p=.029, $p_{corr.}$ = .41, Table 10) and for Ethylmalonic acid ($F_{(1, 351)}$ =4.441, p=.036, $p_{corr.}$ = .43,. Table 11) failed significance after correction of p-vaules. As for the explorative character of the study, a closer look however

shows that children with high SAT values have higher glycine values as compared to both other groups.

Table 10: Glycine in the three SAT-groups

SAT-group	Mean	SD	n
T1	126.37	74.86	118
T2	143.02	89.26	117
T3	151.42	97.23	118
Total	140.26	87.97	353

Abbreviations: n = number of children, SD = Standard Deviation, cases = children in whom succinic acid was found

Ethylmalonic acid was only found in the group with high SAT, while in both groups of lower SAT it was not detected at all, therewith explaining the observed significance.

Table 11: Ethylmalonic acid in the three SAT-groups

SAT-group	Mean	SD	n
T1	0.00	0.00	118
T2	0.00	0.00	117
T3	0.75	4.70	118
Total	0.25	2.73	353

Abbreviations: n = number of children, SD = Standard Deviation, cases = children in whom succinic acid was found

5. Discussion

The present study showed that children grouped by their amount of SAT as an indicator for adiposity differed with regard to the occurrence of metabolites in their urine. The lowest SAT-group exhibited markedly elevated levels of succinic acid and allantoin in the urine as compared to the group with the highest amount of SAT ($p < 0.01$). Similarly, also the second group showed a statistically significant ($p < 0.05$) elevation in succinic acid levels as compared to the third group.

Furthermore, it was determined that girls could be assigned to the SAT group T3 at a notably higher frequency. This observation can be interpreted as an indication that they exhibited a greater level of SAT as compared to boys.

Glycine was observed to be present at a significantly higher level in the group with high SAT compared to the group with lowest SAT, however, applying false discovery rate reduced this effect. Ethylmalonic acid was only detected in the group with high SAT however, given that ethylmalonic acid was identified in only three children, this result is negligible.

5.1 Subcutaneous Adipose Tissue

The minimum of subcutaneous adipose tissue (sum of eight sites) in the total cohort was 10.09 mm, while the maximum was 208.77 mm. The mean value for the total sample was 71.55 mm with a standard deviation of ± 41.99 mm. Measurements of SAT applying the same method and analyses on children in South-Africa aged 7-10 years, revealed a mean value of 47.65 mm with a standard deviation of ± 21.7 mm, while the measured values of the children from Graz were considerably higher and also more widely spread (Schmid-Zalaudek et al., 2021).

Kelso et al. (2019) employed the same methodology to measure subcutaneous adipose tissue on 274 preschool children, aged 4.6 years ± 0.7 in Germany, yielding a mean subcutaneous fat measurement of 46.5 ± 16.3 mm (Kelso et al., 2019). This value is also notably lower than the one observed in the present study, where the children had a mean age of 7.86 ± 1.30 years. Given that the two samples share the same cultural background, and based on the findings of Schmid-Zalaudek et al. (2021) on South African adolescents it might be inferred that subcutaneous adipose tissue increases during the course of development.

It is also noteworthy that the three groups exhibited considerable variation in the measured thickness of subcutaneous fat. While group 1 had a mean value of 33.73 ± 8.53 mm, group 2 a mean value of 60.05 ± 9.04 mm, Group 3 had a mean value of 120.76 ± 33.68 mm with a large variation within the group.

Sex-differences

As demonstrated in Table 5, the regions exhibiting the greatest subcutaneous fat thickness were the upper abdomen, lower abdomen, front thigh, and lateral thigh. Müller et al. identified the lateral thigh measurement point as a particularly salient area in women, given the accumulation of greater subcutaneous fat in this region compared to men (Müller et al., 2016). This region differed also significantly already in children and in adolescents between girls and boys in the study of South-African children (Schmid-Zalaudek et al., 2021). A review of Table 4, which depicts the SAT group allocation in terms of sex, reveals that, in percentage terms, the majority of girls are in group T3, while the majority of boys are in group T1. This suggests that girls tend to have more subcutaneous fat than boys. In a study conducted by Kelso and colleagues, it was observed that even in children with an average age of 4.6 years, there was a notable discrepancy in SAT values between girls and boys (Kelso et al., 2019), which corresponds to our findings.

5.2 Glucose

The presence of glucose was identified in 22% of the total number of urine samples. Of these, 23 samples exhibited a concentration exceeding the established cut-off value of 0.83 mM, and were therefore classified as glucose-positive. It is important to note that these are reference values for adults, as no such values currently exist for children (Gressner, 2013). However, the presence of symptoms associated with glucosuria, including polyuria, polydipsia, and nocturia, serve as confirmed indications of diabetes. Similarly, elevated plasma glucose levels, which are a hallmark of diabetes, lead to an increased proportion of glucose in the urine (American Diabetes Association, 2014).

The prevalence of glucose-positive urine samples in apparently healthy children in this study is strikingly elevated. This prompts the question of whether urine glucose screening for childhood diabetes would be beneficial, as has been conducted in Japan since 1974, for instance. The accuracy of this screening method is up to 50 mg/dL for the detection of

glucose values. Following a positive result, children are advised to visit the hospital for further detailed clarification. This examination has already led to the diagnosis of some children with minimal or no symptoms at an early stage (Urakami et al., 2007).

5.3 Succinic Acid

As early as the 19th century, Robert Koch conducted experiments to study the formation of succinic acid in the human body (Koch, 1865). Although the results of this experiment cannot be accepted without hesitation due to outdated measuring methods, it shows that succinic acid in urine has long been of interest to medicine.

Today we know that succinic acid is a member of the dicarboxylic acid family and plays a role in the citric acid cycle. Consequently, dysregulations of adenosine triphosphate (ATP) synthesis are also associated with those of succinate and occur in certain genetic mitochondrial diseases, including Leigh syndrome and mitochondrial encephalomyopathy with lactic acidosis and stroke-like episodes (MELAS) syndrome. Additionally, succinate has been identified as a contributing factor in the inborn error of metabolism known as D-2-hydroxyglutaric aciduria. In the human body, succinic acid is produced by a number of bacterial species, including Escherichia coli, Pseudomonas aeruginosa, Klebsiella pneumonia, Enterobacter, Acinetobacter, Proteus mirabilis, Citrobacter freundii, and Enterococcus faecalis. Additionally, it is present in Actinobacillus, Anaerobiospirillum, Mannheimia, Corynebacterium, and Basfia (Gupta et al., 2012, Sauer et al., 2008, Becker et al., 2015).

It has been demonstrated that succinate exerts an anti-lipolytic effect on adipose tissue by binding to succinate receptor 1 (Sucnr1) and inhibiting the release of fatty acids from adipocytes (McCreath et al., 2015, Regard et al., 2008). A study conducted in 2018 found a link between increased plasma levels of succinate and obesity. It was also recognized that there is a stronger connection between subcutaneous fat and succinate in plasma than with visceral fat (Serena et al., 2018). The results of this study, in conjunction with our own findings, suggest the possibility of an inverse relationship between plasma and urine succinic acid levels. The lowest levels of succinic acid in urine were observed in subjects with the highest levels of subcutaneous adipose tissue (SAT).

In a study examining the relationship between obesity and changes in urinary metabolites, Elliot and colleagues found an inverse relationship between the amount of urinary succinate and obesity (Elliott et al., 2015). This finding is consistent with the results of the present study, as the amount of succinate was also significantly higher in the group with the least subcutaneous fat than in the group with the most subcutaneous fat. The increased urinary loss of succinate is associated with a small caloric loss of the body, but the main reason for the excretion of tricarboxylic acid (TCA) cycle intermediates may be related to physiological renal function, such as the acid-base balance of the renal tubules. For example, because of the increased utilization of TCA cycle intermediates in the proximal tubular mitochondria, renal tubular acidosis results in decreased excretion of these intermediates (Elliott et al., 2015).

With regard to co-occurrence, our findings indicated that succinic acid was observed in conjunction with acetic acid (6,5%), proline betaine (5,1%), acetoacetic acid (4,1%), methylmalonic acid (4,0%), methanol (3,1%), allantoin (3,0%), 4-aminobutyric acid (2,5%), and L-pyroglutamatic acid (2,1%). While these values appear relatively low, it is not possible to make any statements about their significance at this time.

5.4 Allantoin

Allantoin, also designated as 5-ureidohydantoin or glyoxyldiureide, represents a diureide of glyoxylic acid and is generated through the oxidation of uric acid. Allantoin is a product of purine metabolism in most mammals, with the exception of higher apes, and is present in their urine. The accumulation of loss-of-function mutations in the uricase gene in hominoids results in higher urate concentrations than observed in other mammals. This may have enabled humans to survive environmental stress, evolutionary bottlenecks, and life-threatening pathogens (Roman, 2023). Allantoin has been demonstrated to possess healing, soothing, and anti-irritant properties, which can facilitate the healing of wounds and skin irritations by stimulating the growth of healthy tissue (Xie et al., 2022). It can be isolated from cow urine or as a botanical extract from the comfrey plant and is found in a variety of consumer products, including toothpaste, mouthwash, shampoos, lipsticks, and various cosmetic lotions and creams.

In humans, uric acid is typically excreted instead of allantoin. However, the presence of allantoin in human urine, as observed in all three SAT groups in this study, may indicate microbial overgrowth. Allantoin is a metabolite of Bacillus (Wenzel and Altenbuchner, 2015) and Streptomyces (Zhang et al., 2014). Additionally, it can be produced non-enzymatically by high concentrations of reactive oxygen species. Consequently, allantoin can also be employed as a marker for oxidative stress. A study conducted in 2016, revealed elevated allantoin levels in blood samples obtained from patients diagnosed with Behçet's disease, when compared to those from a control group of healthy individuals. (Yardim-Akaydin et al., 2006). Yang et al. discovered elevated allantoin concentrations in the serum of patients with chronic kidney disease and established a correlation between these levels and the pruritus associated with the disease. In the mouse model, elevated allantoin levels were also identified in the serum, kidney, and urine (Yang et al., 2023).

The impact of allantoin on obesity was examined in a study involving mice fed at high-fat diet. The results demonstrated that chronic allantoin administration for 8 weeks led to a notable reduction in the mice body weight. This outcome is attributed to allantoin's ability to inhibit the imidazoline I_1-receptor (I_1R), which plays a pivotal role in regulating appetite (Chung et al., 2013). These findings are consistent with our results, showing a significantly ($p < 0.01$) lower level of urinary allantoins in the group with high SAT as compared to the group with the lowest SAT. This finding is also consistent with the hypothesis of an inverse relationship between plasma and urine levels of allantoin, as previously observed in studies examining plasma allantoin levels in relation to obesity.

With regard to co-occurrence, our findings indicated that allantoin was observed in conjunction with valine (4,3%), 4-pyidoxic acid (4,1%.), N-isovaleroglycine (3,8%), acetic acid (3,1%), succinic acid (3,0%), syringic acid (2,4%), and methanol (2,3%). As well as in the beforementioned case of succinic acid, these values appear relatively low, and it is not possible to make any statements about their significance at this time.

5.5 Glycine

The name glycine is derived from the Greek word "glucus", which translates to "sweet-tasting". It is a colorless, sweet-tasting crystalline solid that was first identified in 1820 by Henri Braconnot during the hydrolysis of gelatin by boiling with sulfuric acid. Glycine is an

alpha-amino acid and one of the 20 proteinogenic amino acids, which indicates that it is utilized in the biosynthesis of proteins. Glycine is the simplest amino acid and is present in all organisms, from bacteria to plants, and animals. In humans, glycine is a non-essential amino acid, with the average adult consuming 3-5 grams of it daily. In humans, the biosynthesis of glycine occurs from the amino acid serine, which is derived from 3-phosphoglycerate. The synthesis of glycine is catalyzed in the liver by glycine synthase. Additionally, glycine can be derived from threonine, choline, or hydroxyproline through interorgan metabolism involving the liver and kidneys.

Glycine is degraded via three distinct pathways, with the predominant pathway being the reversal of the glycine synthase pathway. Enzymes facilitate the oxidative conversion of glycine into carbon dioxide and ammonia, with the residual one-carbon unit transferred to folate as methylenetetrahydrofolate. This is the most significant pathway for the degradation of glycine (Wishart et al., 2022). In the event of a deficiency in the enzyme system in question, the levels of glycine present in the plasma, urine, and cerebrospinal fluid of patients will be found to be elevated (Van Hove et al., 2005). In patients with diet-controlled phenylketonuria, glycine levels are elevated twofold (Cannet et al., 2023).

Glycine fulfills a multitude of functions within the human body. For example, it is involved in the production of deoxyribonucleic acid (DNA), and hemoglobin as well as in the release of energy. The primary function of glycine is to act as a precursor to proteins; however, the majority of proteins contain only a minimal amount of glycine. Collagen is an exception, as it consists of approximately 35% glycine. Delta-aminolevulinic acid (ALA) is the most significant precursor of porphyrins, which are essential for the synthesis of hemoglobin and cytochrome. ALA is biosynthesized from glycine and succinyl-CoA by the enzyme ALA synthase. Glycine is the central C2N subunit of all purines, which are essential components of ribonucleic acid (RNA) and DNA. Additionally, glycine functions as an inhibitory neurotransmitter within the central nervous system, particularly within spinal cord, brainstem, and retina. Upon activation of glycine receptors, an inhibitory postsynaptic potential is generated through an influx of chloride ions via ionotropic receptors into the neuron (Wishart et al., 2022).

The results of this study indicated that the glycine levels of the group with highest SAT were higher than those of the other groups, though application of the false discovery rate

correction diminished the effect. Still, the results correspond to prior research which has demonstrated that plasma glycine levels are diminished in individuals with obesity and associated conditions, including type 2 diabetes and non-alcoholic fatty liver disease (Guasch-Ferré et al., 2016, Gaggini et al., 2018).

5.6 Sex differences in Urine-Metabolome

With regard to sex, significant differences were identified in the urinary metabolite profile of girls and boys. Acetic acid, D-glucose, succinic acid, and adenine were all present at higher concentrations in the urine of girls. These results provide an impetus for further research in this area. Although there has been research on the differences in the urinary metabolite profile of both sexes, it seems that there is still much to be discovered (Bouatra et al., 2013, Psihogios et al., 2008, Slupsky et al., 2007, Zhang et al., 2012, Liu et al., 2022).

5.7 Limitations

The diagnosis of obesity was based on ultrasound examination of the SAT. Despite the efficacy, reliability and accuracy of this method as well as the involvement of highly trained professionals in the measurement process, the sheer volume of data can potentially introduce some degree of inaccuracy. In six children, not all eight sites of SAT were measured. Consequently, the missing SAT-data were calculated based on the anthropometric data of these six children. While experience has demonstrated that these calculations are highly accurate and the number in relation to the total sample was low, there is still a possibility for error. Furthermore, it should be noted that the method employed in this study is only able to measure subcutaneous and not visceral fat. As the quantity of subcutaneous fat is an unreliable indicator of visceral fat, this was not included in the study.

It is also noteworthy that there is currently no precise definition or cut-off for overweight or obesity for children in relation to the relatively new measurement method used in this study for subcutaneous fat. Consequently, the total population was only divided into three equal groups based on the SAT. Although this allows for the differentiation between children with a low SAT and those with a higher SAT, it is not a precise cut-off for the identification of overweight children and children who are not overweight.

The children's urine was collected between 10 to 11am. Ideally, the urine should have been collected in the morning after an overnight fast to avoid the potential for error due to the consumption of recently ingested foods. However, this was not feasible due to the circumstances.

After collection, the urine was cooled at -80°C and examined after a period of approximately 4 months using NMR spectroscopy. Although there are no exact studies regarding this aspect, it is possible that despite refrigerated storage, changes in the composition of the urine can occur during this period.

5.8 Conclusions

As previously stated, differences in the urinary metabolite profile were observed between children with low and high levels of subcutaneous fat. A total of three metabolites were identified, namely succinic acid, allantoin, and glycine, which may be pertinent in the context of childhood obesity. Given the diverse roles of these metabolites in the human body and the relatively novel research field of urine metabolomics, further studies are necessary to ascertain the precise association of these metabolites with obesity. The discrepancies between the sexes with regard to the SAT have been discerned. The data collected substantiates the second hypothesis of this study, indicating that girls tend to have higher SAT scores than boys.

5.9 Perspectives

The prevalence of childhood obesity continues to increase. It is imperative that greater attention be devoted to the implementation of comprehensive health programs within educational institutions, coupled with enhanced research initiatives and heightened awareness of the prevalence of childhood obesity. Regardless of the underlying cause, all children should undergo screening for lifestyle risk factors and complications associated with obesity should be identified as expeditiously as possible. In the future, the identification of obesity by means of a urine test may represent a non-invasive option for early diagnosis. Nevertheless, further research is required to establish precise criteria for this. For example, future studies should also concentrate on alterations in urinary metabolites resulting from intervention.

6. References

ACKLAND, T. R., LOHMAN, T. G., SUNDGOT-BORGEN, J., MAUGHAN, R. J., MEYER, N. L., STEWART, A. D. & MÜLLER, W. 2012. Current status of body composition assessment in sport: review and position statement on behalf of the ad hoc research working group on body composition health and performance, under the auspices of the I.O.C. Medical Commission. *Sports Medicine,* 42**,** 227-49.

ADOM, T., KENGNE, A. P., DE VILLIERS, A., BOATIN, R. & PUOANE, T. 2020. Diagnostic accuracy of body mass Index in defining childhood obesity: analysis of cross-sectional data from Ghanaian children. *International Journal of Environmental Research and Public Health,* 17**,** 36.

ALBERTI, K. G. M., ZIMMET, P. & SHAW, J. 2005. The metabolic syndrome—a new worldwide definition. *The Lancet,* 366**,** 1059-1062.

ALI, O., CERJAK, D., KENT JR, J., JAMES, R., BLANGERO, J. & ZHANG, Y. 2014. Obesity, central adiposity and cardiometabolic risk factors in children and adolescents: a family-based study. *Pediatric Obesity,* 9**,** 58-62.

AMERICAN DIABETES ASSOCIATION 2014. Executive summary: Standards of medical care in diabetes--2014. *Diabetes Care,* 37 S5-13.

ANDERHUBER, F., PERA, F. & STREICHER, J. 2012. *Waldeyer - Anatomie des Menschen,* Berlin, Boston, De Gruyter.

ARNER, P. 1997. Obesity and the adipocyte. Regional adipocity in man. *J Endocrinol,* 155**,** 191-192.

BECKER, J., LANGE, A., FABARIUS, J. & WITTMANN, C. 2015. Top value platform chemicals: bio-based production of organic acids. *Current Opinion in Biotechnology,* 36**,** 168-75.

BEREKET, A., KIESS, W., LUSTIG, R., MULLER, H., GOLDSTONE, A., WEISS, R., YAVUZ, Y. & HOCHBERG, Z. 2012. Hypothalamic obesity in children. *Obesity Reviews,* 13**,** 780-798.

BHAWANA, A. & VANDANA, J. 2018. Obesity in Children: Definition, Etiology and Approach. *Indian Journal of Pedriatics,* 85**,** 463-471.

BOUATRA, S., AZIAT, F., MANDAL, R., GUO, A. C., WILSON, M. R., KNOX, C., BJORNDAHL, T. C., KRISHNAMURTHY, R., SALEEM, F. & LIU, P. 2013. The human urine metabolome. *PloS one,* 8**,** e73076.

BOWMAN, S. A., GORTMAKER, S. L., EBBELING, C. B., PEREIRA, M. A. & LUDWIG, D. S. 2004. Effects of fast-food consumption on energy intake and diet quality among children in a national household survey. *Pediatrics,* 113**,** 112-118.

BUDDE, K., GÖK, Ö.-N., PIETZNER, M., MEISINGER, C., LEITZMANN, M., NAUCK, M., KÖTTGEN, A. & FRIEDRICH, N. 2016. Quality assurance in the pre-analytical phase of human urine samples by 1H NMR spectroscopy. *Archives of Biochemistry and Biophysics,* 589**,** 10-17.

BUJAK, R., STRUCK-LEWICKA, W., MARKUSZEWSKI, M. J. & KALISZAN, R. 2015. Metabolomics for laboratory diagnostics. *Journal of Pharmaceutical and Biomedical Analysis,* 113**,** 108-120.

CANNET, C., BAYAT, A., FRAUENDIENST-EGGER, G., FREISINGER, P., SPRAUL, M., HIMMELREICH, N., KOCKAYA, M., AHRING, K., GODEJOHANN, M. & MACDONALD, A. 2023. Phenylketonuria (PKU) Urinary Metabolomic Phenotype Is Defined by Genotype and Metabolite Imbalance: Results in 51 Early Treated Patients Using Ex Vivo 1H-NMR Analysis. *Molecules,* 28.

CHUMELA, W. & SUN, S. 2005. Bioelectrical impedance analysis. *In:* HEYMSFIELD, S. B., LOHMAN, T. G., WANG, Z. & GOING, S. B. (eds.) *Human Body Composition.* 2 ed. Champaign: Human Kinetics.

CHUNG, H.-H., LEE, K. S. & CHENG, J.-T. 2013. Decrease of Obesity by Allantoin via Imidazoline I1-Receptor Activation in High Fat Diet-Fed Mice. *Evidence-Based Complementary and Alternative Medicine,* 2013**,** 589309.

CLARYS, J. P., SCAFOGLIERI, A., PROVYN, S., LOUIS, O., WALLACE, J. A. & DE MEY, J. 2010. A macro-quality evaluation of DXA variables using whole dissection, ashing, and computer tomography in pigs. *Obesity,* 18**,** 1477.

COLE, T. J., BELLIZZI, M. C., FLEGAL, K. M. & DIETZ, W. H. 2000. Establishing a standard definition for child overweight and obesity worldwide: international survey. *BMJ,* 320.

COOK, S., WEITZMAN, M., AUINGER, P., NGUYEN, M. & DIETZ, W. H. 2003. Prevalence of a metabolic syndrome phenotype in adolescents: findings from the third National Health and Nutrition Examination Survey, 1988-1994. *Archives of pediatrics & adolescent medicine,* 157**,** 821-827.

CRINO, A., GREGGIO, N., BECCARIA, L., SCHIAFFINI, R., PIETROBELLI, A. & MAFFEIS, C. 2003. Diagnosis and differential diagnosis of obesity in childhood. *Minerva Pediatrica,* 55**,** 461-470.

CROCKER, M. K. & YANOVSKI, J. A. 2009. Pediatric obesity: etiology and treatment. *Endocrinology and Metabolism Clinics,* 38**,** 525-548.

CUTTING, T. M., FISHER, J. O., GRIMM-THOMAS, K. & BIRCH, L. L. 1999. Like mother, like daughter: familial patterns of overweight are mediated by mothers' dietary disinhibition. *The American Journal of Clinical Nutrition,* 69**,** 608-613.

DELISLE NYSTRÖM, C., HENRIKSSON, P., EK, A., HENRIKSSON, H., ORTEGA, F. B., RUIZ, J. R. & LÖF, M. 2018. Is BMI a relevant marker of fat mass in 4 year old children? Results from the MINISTOP trial. *European Journal of Clinical Nutrition,* 72**,** 1561-1566.

DURNIN, J. V. & WOMERSLEY, J. 1974. Body fat assessed from total body density and its estimation from skinfold thickness: measurements on 481 men and women aged from 16 to 72 years. *British Journal of Nutrition,* 32**,** 77-97.

ELLIOTT, P., POSMA, J. M., CHAN, Q., GARCIA-PEREZ, I., WIJEYESEKERA, A., BICTASH, M., D. EBBELS, T. M., UESHIMA, H., ZHAO, L. & VAN HORN, L. 2015. Urinary metabolic signatures of human adiposity. *Science Translational Medicine,* 7**,** 285ra62-285ra62.

FAROOQI, I. S. & O'RAHILLY, S. 2005. Monogenic obesity in humans. *Annual Review od Medicine,* 56**,** 443-458.

FREDRIKSEN, P. M., HJELLE, O. P., MAMEN, A., MEZA, T. J. & WESTERBERG, A. C. 2017. The health Oriented pedagogical project (HOPP)-a controlled longitudinal school-based physical activity intervention program. *BMC Public Health*.

FRENCH, S. A. & WECHSLER, H. 2004. School-based research and initiatives: fruit and vegetable environment, policy, and pricing workshop. *Preventive medicine,* 39**,** 101-107.

FRIEBOLIN, H. 2013. *Ein-und zweidimensionale NMR-Spektroskopie: eine Einführung,* Weinheim, John Wiley & Sons.

GAGGINI, M., CARLI, F., ROSSO, C., BUZZIGOLI, E., MARIETTI, M., DELLA LATTA, V., CIOCIARO, D., ABATE, M. L., GAMBINO, R. & CASSADER, M. 2018. Altered amino acid concentrations in NAFLD: Impact of obesity and insulin resistance. *Hepatology,* 67**,** 145-158.

GOH, K.-I., CUSICK, M. E., VALLE, D., CHILDS, B., VIDAL, M. & BARABÁSI, A.-L. 2007. The human disease network. *Proceedings of the National Academy of Sciences,* 104**,** 8685-8690.

GONZÁLEZ-ÁLVAREZ, C., RAMOS-IBÁÑEZ, N., AZPRIOZ-LEEHAN, J. & ORTIZ-HERNÁNDEZ, L. 2017. Intra-abdominal and subcutaneous abdominal fat as predictors of cardiometabolic risk in a sample of Mexican children. *European Journal of Clinical Nutrition,* 71**,** 1068-1073.

GOSWAMI, N., HANSEN, D., GUMZE, G., BRIX, B., SCHMID-ZALAUDEK, K. & FREDRIKSEN, P. M. 2022. Health and Academic Performance With Happy Children: A Controlled Longitudinal Study Based on the HOPP Project. *Frontiers in Cardiovascular Medicine*.

GRESSNER, A. 2013. *Lexikon der Medizinischen Labordiagnostik,* Berlin, Springer.

GRIFFITH, D. M., VEECH, J. A. & MARSH, C. J. 2016. cooccur: Probabilistic Species Co-Occurrence Analysis in R. *Journal of Statistical Software,* 69**,** 1 - 17.

GUASCH-FERRÉ, M., HRUBY, A., TOLEDO, E., CLISH, C. B., MARTÍNEZ-GONZÁLEZ, M. A., SALAS-SALVADÓ, J. & HU, F. B. 2016. Metabolomics in prediabetes and diabetes: a systematic review and meta-analysis. *Diabetes Care,* 39**,** 833-846.

GUPTA, A., DWIVEDI, M., MAHDI, A. A., KHETRAPAL, C. L. & BHANDARI, M. 2012. Broad identification of bacterial type in urinary tract infection using (1)h NMR spectroscopy. *Journal of Proteome Research,* 11**,** 1844-54.

HILL, J. O. & PETERS, J. C. 1998. Environmental contributions to the obesity epidemic. *Science,* 280**,** 1371-1374.

HORN, F., MOC, I., ZIEGLER, P., BERGHOLD, S., ARMBRUSTER, M. & GRILLHÖSL, C. 2015. *Biochemie des Menschen,* Stuttgart, Thieme.

HORNING, E. & HORNING, M. 1971a. Human metabolic profiles obtained by GC and GC/MS. *Journal of Chromatographic Science,* 9**,** 129-140.

HORNING, E. & HORNING, M. 1971b. Metabolic profiles: gas-phase methods for analysis of metabolites. *Clinical Chemistry,* 17**,** 802-809.

HUME, P. & MARFELL-JONES, M. 2008. The importance of accurate site location for skinfold measurement. *Journal of Sports Sciences,* 26**,** 1333-1340.

JARNIG, G., KERBL, R., JAUNIG, J. & VAN POPPEL, M. N. 2023. Effects of a daily physical activity intervention on the health-related fitness status of primary school children: A cluster randomized controlled trial. *Journal of Sports Sciences,* 41**,** 1073-1082.

JAVED, A., JUMEAN, M., MURAD, M. H., OKORODUDU, D., KUMAR, S., SOMERS, V., SOCHOR, O. & LOPEZ-JIMENEZ, F. 2015. Diagnostic

performance of body mass index to identify obesity as defined by body adiposity in children and adolescents: a systematic review and meta-analysis. *Pediatric Obesity,* 10**,** 234-244.

JENSEN, N. S., CAMARGO, T. F. & BERGAMASCHI, D. P. 2016. Comparison of methods to measure body fat in 7-to-10-year-old children: a systematic review. *Public Health,* 133**,** 3-13.

JOHNSON, S. L. & BIRCH, L. L. 1994. Parents' and children's adiposity and eating style. *Pediatrics,* 94**,** 653-661.

KELLY, A. S., DENGEL, D. R., HODGES, J., ZHANG, L., MORAN, A., CHOW, L., SINAIKO, A. R. & STEINBERGER, J. 2014. The relative contributions of the abdominal visceral and subcutaneous fat depots to cardiometabolic risk in youth. *Clinical Obesity,* 4**,** 101-107.

KELSO, A., MÜLLER, W., FÜRHAPTER-RIEGER, A., SENGEIS, M., AHAMMER, H. & STEINACKER, J. M. 2020. High inter-observer reliability in standardized ultrasound measurements of subcutaneous adipose tissue in children aged three to six years. *BMC Pediatrics,* 20**,** 145.

KELSO, A., VOGEL, K. & STEINACKER, J. M. 2019. Ultrasound measurements of subcutaneous adipose tissue thickness show sexual dimorphism in children of three to five years of age. *Acta Paediatrica,* 108**,** 514-521.

KIM, H.-J., KIM, J. H., NOH, S., HUR, H. J., SUNG, M. J., HWANG, J.-T., PARK, J. H., YANG, H. J., KIM, M.-S. & KWON, D. Y. 2011. Metabolomic analysis of livers and serum from high-fat diet induced obese mice. *Journal of Proteome Research,* 10**,** 722-731.

KIM, S.-H., YANG, S.-O., KIM, H.-S., KIM, Y., PARK, T. & CHOI, H.-K. 2009. 1 H-nuclear magnetic resonance spectroscopy-based metabolic assessment in a rat model of obesity induced by a high-fat diet. *Analytical and Bioanalytical Chemistry,* 395**,** 1117-1124.

KJELLBERG, E., ROSWALL, J., ANDERSSON, J., BERGMAN, S., KARLSSON, A. K., SVENSSON, P. A., KULLBERG, J. & DAHLGREN, J. 2019. Metabolic risk factors associated with visceral and subcutaneous adipose tissue in a sex-specific manner in seven-year-olds. *Obesity,* 27**,** 982-988.

KOCH, R. 1865. Über das Entstehen der Bernsteinsäure im menschlichen Organismus. *Zeitschrift für rationelle Medizin,* 24.

LEAL-WITT, M. J., LLOBET, M., SAMINO, S., CASTELLANO, P., CUADRAS, D., JIMENEZ-CHILLARON, J. C., YANES, O., RAMON-KRAUEL, M. & LERIN, C. 2018. Lifestyle Intervention Decreases Urine Trimethylamine N-Oxide Levels in Prepubertal Children with Obesity. *Obesity (Silver Spring),* 26**,** 1603-1610.

LEE, J. J., PEDLEY, A., THERKELSEN, K. E., HOFFMANN, U., MASSARO, J. M., LEVY, D. & LONG, M. T. 2017. Upper body subcutaneous fat is associated with cardiometabolic risk factors. *The American Journal of Medicine,* 130**,** 958-966. e1.

LEE, Y., CHO, J.-Y. & CHO, K. Y. 2023. Serum, Urine, and Fecal Metabolome Alterations in the Gut Microbiota in Response to Lifestyle Interventions in Pediatric Obesity: A Non-Randomized Clinical Trial. *Nutrients,* 15.

LIU, F., GAN, P. P., WU, H., WOO, W. S., ONG, E. S. & LI, S. F. Y. 2012. A combination of metabolomics and metallomics studies of urine and serum from hypercholesterolaemic rats after berberine injection. *Analytical and Bioanalytical Chemistry,* 403**,** 847-856.

LIU, J., FOX, C. S., HICKSON, D. A., MAY, W. D., HAIRSTON, K. G., CARR, J. J. & TAYLOR, H. A. 2010. Impact of abdominal visceral and subcutaneous adipose tissue on cardiometabolic risk factors: the Jackson Heart Study. *The Journal of Clinical Endocrinology & Metabolism,* 95**,** 5419-5426.

LIU, X., TIAN, X., QINGHONG, S., SUN, H., JING, L., TANG, X., GUO, Z., LIU, Y., WANG, Y., MA, J., NA, R., HE, C., SONG, W. & SUN, W. 2022. Characterization of LC-MS based urine metabolomics in healthy children and adults. *PeerJ,* 10**,** 13545.

LOHMAN, T. G. 1992. Advances in human body composition. *Human Kinetics*.

LOHMAN, T. G., ROCHE, A. F. & MARTORELL, R. 1988. Anthropometric standardization reference manual. *Human Kinetics.* Champaign.

LU, C., ZHAO, X., LI, Y., LI, Y., YUAN, C., XU, F., MENG, X., HOU, L. & XU, G. 2016. Serum metabolomics study of Traditional Chinese medicine formula intervention to polycystic ovary syndrome. *Journal of pharmaceutical and biomedical analysis,* 120**,** 127-133.

LÜLLMANN-RAUCH, R. & PAULSEN, F. 2019. *Taschenlehrbuch Histologie,* Stuttgart, Thieme.

MAMUN, A. A., LAWLOR, D. A., CRAMB, S., O'CALLAGHAN, M., WILLIAMS, G. & NAJMAN, J. 2007. Do childhood sleeping problems predict obesity in young

adulthood? Evidence from a prospective birth cohort study. *American Journal of Epidemiology,* 166**,** 1368-1373.

MARFELL-JONES, M., OLDS, T., STEWART, A. & CARTER, L. 2006. *International standards for anthropometric assessment (2006),* Potchesfstroom, International Society for the Advancement of Kinanthropometry (ISAK).

MÅRIN, P., ANDERSSON, B., OTTOSSON, M., OLBE, L., CHOWDHURY, B., KVIST, H., HOLM, G., SJÖSTRÖM, L. & BJÖRNTORP, P. 1992. The morphology and metabolism of intraabdominal adipose tissue in men. *Metabolism,* 41**,** 1242-1248.

MASON, K., PAGE, L. & BALIKCIOGLU, P. G. 2014. Screening for hormonal, monogenic, and syndromic disorders in obese infants and children. *Pediatric Annals,* 43**,** 218-224.

MATSHA, T. E., ISMAIL, S., SPEELMAN, A., HON, G. M., DAVIDS, S., ERASMUS, R. T. & KENGNE, A. P. 2019. Visceral and subcutaneous adipose tissue association with metabolic syndrome and its components in a South African population. *Clinical Nutrition ESPEN,* 32**,** 76-81.

MCCARTHY, H., COLE, T., FRY, T., JEBB, S. & PRENTICE, A. 2006. Body fat reference curves for children. *International Journal of Obesity,* 30**,** 598-602.

MCCREATH, K. J., ESPADA, S., GÁLVEZ, B. G., BENITO, M., DE MOLINA, A., SEPÚLVEDA, P. & CERVERA, A. M. 2015. Targeted disruption of the SUCNR1 metabolic receptor leads to dichotomous effects on obesity. *Diabetes,* 64**,** 1154-1167.

MEN, L., PI, Z., ZHOU, Y., WEI, M., LIU, Y., SONG, F. & LIU, Z. 2017. Urine metabolomics of high-fat diet induced obesity using UHPLC-Q-TOF-MS. *Journal of Pharmaceutical and Biomedical Analysis,* 132**,** 258-266.

MISRA, A. & VIKRAM, N. K. 2003. Clinical and pathophysiological consequences of abdominal adiposity and abdominal adipose tissue depots. *Nutrition,* 19**,** 457-466.

MOHSEN, I. M. 2009. Subcutaneous and visceral adipose tissue:
structural and functional differences. *Obesity Reviews,* 11**,** 11-18.

MONASTA, L., LOBSTEIN, T., COLE, T., VIGNEROVÁ, J. & CATTANEO, A. 2011. Defining overweight and obesity in pre-school children: IOTF reference or WHO standard? *Obesity Reviews,* 12**,** 295-300.

MÜLLER, W., FÜRHAPTER-RIEGER, A., AHAMMER, H., LOHMAN, T. G., MEYER, N. L., SARDINHA, L. B., STEWART, A. D., MAUGHAN, R. J., SUNDGOT-

BORGEN, J., MÜLLER, T., HARRIS, M., KIRIHENNEDIGE, N., MAGALHAES, J. P., MELO, X., PIRSTINGER, W., REGUANT-CLOSA, A., RISOUL-SALAS, V. & ACKLAND, T. R. 2020. Relative Body Weight and Standardised Brightness-Mode Ultrasound Measurement of Subcutaneous Fat in Athletes: An International Multicentre Reliability Study, Under the Auspices of the IOC Medical Commission. *Sports Med,* 50**,** 597-614.

MÜLLER, W., LOHMAN, T. G., STEWART, A. D., MAUGHAN, R. J., MEYER, N. L., SARDINHA, L. B., KIRIHENNEDIGE, N., REGUANT-CLOSA, A., RISOUL-SALAS, V., SUNDGOT-BORGEN, J., AHAMMER, H., ANDERHUBER, F., FÜRHAPTER-RIEGER, A., KAINZ, P., MATERNA, W., PILSL, U., PIRSTINGER, W. & ACKLAND, T. R. 2016. Subcutaneous fat patterning in athletes: selection of appropriate sites and standardisation of a novel ultrasound measurement technique: ad hoc working group on body composition, health and performance, under the auspices of the IOC Medical Commission. *British Journal of Sports Medicine,* 50**,** 45-54.

NAZARE, J.-A., SMITH, J. D., BOREL, A.-L., HAFFNER, S. M., BALKAU, B., ROSS, R., MASSIEN, C., ALMÉRAS, N. & DESPRÉS, J.-P. 2012. Ethnic influences on the relations between abdominal subcutaneous and visceral adiposity, liver fat, and cardiometabolic risk profile: the International Study of Prediction of Intra-Abdominal Adiposity and Its Relationship With Cardiometabolic Risk/Intra-Abdominal Adiposity. *The American Journal of Clinical Nutrition,* 96**,** 714-726.

OKORODUDU, D. O., JUMEAN, M., MONTORI, V. M., ROMERO-CORRAL, A., SOMERS, V. K., ERWIN, P. J. & LOPEZ-JIMENEZ, F. 2010. Diagnostic performance of body mass index to identify obesity as defined by body adiposity: a systematic review and meta-analysis. *International Journal of Obesity,* 34**,** 791-799.

ONIS, M. D., ONYANGO, A. W., BORGHI, E., SIYAM, A., NISHIDA, C. & SIEKMANN, J. 2007. Development of a WHO growth reference for school-aged children and adolescents. *Bulletin of the World Health Organization,* 85**,** 660-667.

PANG, Z., LU, Y., ZHOU, G., HUI, F., XU, L., VIAU, C., SPIGELMAN, ALIYA F., MACDONALD, PATRICK E., WISHART, DAVID S., LI, S. & XIA, J. 2024. MetaboAnalyst 6.0: towards a unified platform for metabolomics data processing, analysis and interpretation. *Nucleic Acids Research,* 52**,** W398-W406.

PAPE, H.-C., KURTZ, A. & SILBERNAGL, S. 2014. *Physiologie,* Stuttgart, Thieme.

PAULING, L., ROBINSON, A. B., TERANISHI, R. & CARY, P. 1971. Quantitative analysis of urine vapor and breath by gas-liquid partition chromatography. *Proceedings of the National Academy of Sciences,* 68**,** 2374-2376.

PSIHOGIOS, N. G., GAZI, I. F., ELISAF, M. S., SEFERIADIS, K. I. & BAIRAKTARI, E. T. 2008. Gender-related and age-related urinalysis of healthy subjects by NMR-based metabonomics. *NMR in Biomedicine: An International Journal Devoted to the Development and Application of Magnetic Resonance In vivo,* 21**,** 195-207.

PULGARÓN, E. R. 2013. Childhood obesity: a review of increased risk for physical and psychological comorbidities. *Clinical Therapeutics,* 35**,** A18-A32.

RANASINGHE, P., JAYAWARDENA, R., GAMAGE, N., PUJITHA WICKRAMASINGHE, V. & HILLS, A. P. 2021. The range of non-traditional anthropometric parameters to define obesity and obesity-related disease in children: a systematic review. *European Journal of Clinical Nutrition,* 75**,** 373-384.

REGARD, J. B., SATO, I. T. & COUGHLIN, S. R. 2008. Anatomical profiling of G protein-coupled receptor expression. *Cell,* 135**,** 561-571.

REILLY, J. J. & KELLY, J. 2011. Long-term impact of overweight and obesity in childhood and adolescence on morbidity and premature mortality in adulthood: systematic review. *International journal of obesity,* 35**,** 891-898.

ROMAN, Y. M. 2023. The role of uric acid in human health: insights from the uricase gene. *Journal of Personalized Medicine,* 13**,** 1409.

ROTHMAN, K. J. 2008. BMI-related errors in the measurement of obesity. *International Journal of Obesity,* 32**,** 56-59.

SAUER, M., PORRO, D., MATTANOVICH, D. & BRANDUARDI, P. 2008. Microbial production of organic acids: expanding the markets. *Trends Biotechnol,* 26**,** 100-8.

SCHMID-ZALAUDEK, K., BRIX, B., SENGEIS, M., JANTSCHER, A., FÜRHAPTER-RIEGER, A., MÜLLER, W., MATJUDA, E. N., MUNGAMBA, M. M., NKEH-CHUNGAG, B., FREDRIKSEN, P. M. & GOSWAMI, N. 2021. Subcutaneous Adipose Tissue Measured by B-Mode Ultrasound to Assess and Monitor Obesity and Cardio-Metabolic Risk in Children and Adolescents. *Biology (Basel),* 10.

SENGEIS, M., MÜLLER, W., STÖRCHLE, P. & FÜHRHAPTER-RIEGER, A. 2019. Body weight and subcutaneous fat patterning in elite judokas. *Scandinavian Journal of Medicine & Science in Sports,* 29**,** 1774-1788.

SERENA, C., CEPERUELO-MALLAFRÉ, V., KEIRAN, N., QUEIPO-ORTUÑO, M. I., BERNAL, R., GOMEZ-HUELGAS, R., URPI-SARDA, M., SABATER, M.,

PÉREZ-BROCAL, V. & ANDRÉS-LACUEVA, C. 2018. Elevated circulating levels of succinate in human obesity are linked to specific gut microbiota. *The ISME journal,* 12**,** 1642-1657.

SHAH, P., MISRA, A., GUPTA, N., HAZRA, D. K., GUPTA, R., SETH, P., AGARWAL, A., GUPTA, A. K., JAIN, A. & KULSHRESHTA, A. 2010. Improvement in nutrition-related knowledge and behaviour of urban Asian Indian school children: findings from the 'Medical education for children/Adolescents for Realistic prevention of obesity and diabetes and for healthy aGeing'(MARG) intervention study. *British Journal of Nutrition,* 104**,** 427-436.

SHEARER, J., DUGGAN, G., WELJIE, A., HITTEL, D., WASSERMAN, D. & VOGEL, H. 2008. Metabolomic profiling of dietary-induced insulin resistance in the high fat–fed C57BL/6J mouse. *Diabetes, Obesity and Metabolism,* 10**,** 950-958.

SIMONI, P., GUGLIELMI, R. & GÓMEZ, M. P. A. 2020. Imaging of body composition in children. *Quantitative Imaging in Medicine and Surgery,* 10**,** 1661.

SLICHTER, C. P. 1963. *Principles of Magnetic Resonance: With Examples from Solid State Physics,* New York, Springer.

SLUPSKY, C. M., RANKIN, K. N., WAGNER, J., FU, H., CHANG, D., WELJIE, A. M., SAUDE, E. J., LIX, B., ADAMKO, D. J. & SHAH, S. 2007. Investigations of the effects of gender, diurnal variation, and age in human urinary metabolomic profiles. *Analytical Chemistry,* 79**,** 6995-7004.

SPRUIJT-METZ, D., LINDQUIST, C. H., BIRCH, L. L., FISHER, J. O. & GORAN, M. I. 2002. Relation between mothers' child-feeding practices and children's adiposity. *The American Journal of Clinical Nutrition,* 75**,** 581-586.

SRIKANTHA, P. & MOHAJERI, M. H. 2019. The Possible Role of the Microbiota-Gut-Brain-Axis in Autism Spectrum Disorder. *International Journal of Molecular Sciences,* 20**,** 2115.

STÖRCHLE, P., MÜLLER, W., SENGEIS, M., AHAMMER, H., FÜRHAPTER-RIEGER, A., BACHL, N., LACKNER, S., MÖRKL, S. & HOLASEK, S. 2017. Standardized Ultrasound Measurement of Subcutaneous Fat Patterning: High Reliability and Accuracy in Groups Ranging from Lean to Obese. *Ultrasound in medicine and biology,* 43**,** 427-438.

STRYECK, S., HORVATH, A., LEBER, B., STADLBAUER, V. & MADL, T. 2018. NMR spectroscopy enables simultaneous quantification of carbohydrates for diagnosis of intestinal and gastric permeability. *Scientific reports,* 8**,** 14650.

STURM, D. J., KELSO, A., KOBEL, S. & DEMETRIOU, Y. 2020. Physical activity levels and sedentary time during school hours of 6th-grade girls in Germany. *Journal of Public Health,* 29**,** 847-855.

SWINBURN, B., EGGER, G. & RAZA, F. 1999. Dissecting obesogenic environments: the development and application of a framework for identifying and prioritizing environmental interventions for obesity. *Preventive medicine,* 29**,** 563-570.

URAKAMI, T., MORIMOTO, S., NITADORI, Y., HARADA, K., OWADA, M. & KITAGAWA, T. 2007. Urine Glucose Screening Program at Schools in Japan to Detect Children with Diabetes and Its Outcome-Incidence and Clinical Characteristics of Childhood Type 2 Diabetes in Japan. *Pediatric Research,* 61**,** 141-145.

VAN HOVE, J., KERCKHOVE, K. V., HENNERMANN, J., MAHIEU, V., DECLERCQ, P., MERTENS, S., DE BECKER, M., KISHNANI, P. & JAEKEN, J. 2005. Benzoate treatment and the glycine index in nonketotic hyperglycinaemia. *Journal of Inherited Metabolic Disease,* 28**,** 651-663.

VANDERWALL, C., RANDALL CLARK, R., EICKHOFF, J. & CARREL, A. L. 2017. BMI is a poor predictor of adiposity in young overweight and obese children. *BMC Pediatrics,* 17**,** 1-6.

WAJCHENBERG, B. L. O. 2000. Subcutaneous and Visceral Adipose Tissue: Their Relation to the Metabolic Syndrome. *Endocrine Reviews,* 21**,** 697-738.

WANG, Z., HEYMSFIELD, S. B., CHEN, Z., ZHU, S. & PIERSON, R. N. 2010. Estimation of percentage body fat by dual-energy x-ray absorptiometry: evaluation by in vivo human elemental composition. *Physics in Medicine & Biology,* 55**,** 2619.

WEI, H., PASMAN, W., RUBINGH, C., WOPEREIS, S., TIENSTRA, M., SCHROEN, J., WANG, M., VERHEIJ, E. & VAN DER GREEF, J. 2012. Urine metabolomics combined with the personalized diagnosis guided by Chinese medicine reveals subtypes of pre-diabetes. *Molecular BioSystems,* 8**,** 1482-1491.

WEIHE, P. & WEIHRAUCH-BLÜHER, S. 2019. Metabolic Syndrome in Children and Adolescents: Diagnostic Criteria, Therapeutic Options and Perspectives. *Current Obesity Reports,* 8**,** 472-479.

WELSCH, U., KUMMER, W. & DELLER, T. 2022. *Histologie: Lehrbuch und Atlas,* München, Elsevier.

WENZEL, M. & ALTENBUCHNER, J. 2015. Development of a markerless gene deletion system for Bacillus subtilis based on the mannose phosphoenolpyruvate-dependent phosphotransferase system. *Microbiology,* 161**,** 1942-1949.

WHO. 2017. *Seventieth World Health Assembly: Report of the Commission on Ending Childhood Obesity: Implementation Plan* [Online]. Available: https://apps.who.int/gb/ebwha/pdf_files/WHA70/A70_31-en.pdf [Accessed 17.05.2022].

WHO 2021. The UNICEF/WHO/WB Joint Child Matnutrion Estimates (JME). Geneva: WHO.

WHO, C. 2000. *Obesity: preventing and managing the global epidemic,* Geneva, World Health Organization.

WHO, M. G. R. S. G. 2006. WHO Child Growth Standards based on length/height, weight and age. *Acta Paediatrica,* 450**,** 76-85.

WICKRAMASINGHE, V., CLEGHORN, G., EDMISTON, K., MURPHY, A., ABBOTT, R. & DAVIES, P. 2005. Validity of BMI as a measure of obesity in Australian white Caucasian and Australian Sri Lankan children. *Annals of Human Biology,* 32**,** 60-71.

WILLIAMS, P. G., HOLMBECK, G. N. & GREENLEY, R. N. 2002. Adolescent health psychology. *Journal of Consulting and Clinical Psychology,* 70**,** 828.

WISHART, D. S., GUO, A., OLER, E., WANG, F., ANJUM, A., PETERS, H., DIZON, R., SAYEEDA, Z., TIAN, S., LEE, B. L., BERJANSKII, M., MAH, R., YAMAMOTO, M., JOVEL, J., TORRES-CALZADA, C., HIEBERT-GIESBRECHT, M., LUI, V. W., VARSHAVI, D., VARSHAVI, D., ALLEN, D., ARNDT, D., KHETARPAL, N., SIVAKUMARAN, A., HARFORD, K., SANFORD, S., YEE, K., CAO, X., BUDINSKI, Z., LIIGAND, J., ZHANG, L., ZHENG, J., MANDAL, R., KARU, N., DAMBROVA, M., SCHIÖTH, H. B., GREINER, R. & GAUTAM, V. 2022. The human metabolome database (HMDB). *Nucleic Acids Research,* 50**,** D622-d631.

XIE, H., BAI, Q., KONG, F., LI, Y., ZHA, X., ZHANG, L., ZHAO, Y., GAO, S., LI, P. & JIANG, Q. 2022. Allantoin-functionalized silk fibroin/sodium alginate transparent scaffold for cutaneous wound healing. *International Journal of Biological Macromolecules,* 207**,** 859-872.

YAN, Y., LIU, J., ZHAO, X., CHENG, H., HUANG, G. & MI, J. 2019. Abdominal visceral and subcutaneous adipose tissues in association with cardiometabolic risk

in children and adolescents: the China Child and Adolescent Cardiovascular Health (CCACH) study. *BMJ Open Diabetes Research and Care,* 7**,** e000824.

YANG, Y., SUN, Y., ZHU, C., SHEN, X., SUN, J., JING, T., JUN, S., WANG, C., YU, G. & DONG, X. 2023. Allantoin induces pruritus by activating MrgprD in chronic kidney disease. *Journal of Cellular Physiology,* 238**,** 813-828.

YARDIM-AKAYDIN, S., SEPICI, A., ÖZKAN, Y., ŞIMŞEK, B. & SEPICI, V. 2006. Evaluation of allantoin levels as a new marker of oxidative stress in Behçet's disease. *Scandinavian Journal of Rheumatology,* 35**,** 61-64.

ZHANG, C., YIN, A., LI, H., WANG, R., WU, G., SHEN, J., ZHANG, M., WANG, L., HOU, Y., OUYANG, H., ZHANG, Y., ZHENG, Y., WANG, J., LV, X., WANG, Y., ZHANG, F., ZENG, B., LI, W., YAN, F., ZHAO, Y., PANG, X., ZHANG, X., FU, H., CHEN, F., ZHAO, N., HAMAKER, B. R., BRIDGEWATER, L. C., WEINKOVE, D., CLEMENT, K., DORE, J., HOLMES, E., XIAO, H., ZHAO, G., YANG, S., BORK, P., NICHOLSON, J. K., WEI, H., TANG, H., ZHANG, X. & ZHAO, L. 2015. Dietary Modulation of Gut Microbiota Contributes to Alleviation of Both Genetic and Simple Obesity in Children. *EBioMedicine,* 2**,** 968-84.

ZHANG, S., LIU, L., STEFFEN, D., YE, T. & RAFTERY, D. 2012. Metabolic profiling of gender: Headspace-SPME/GC–MS and 1 H NMR analysis of urine. *Metabolomics,* 8**,** 323-334.

ZHANG, Y., XU, P., LI, W. & TAO, Y. 2014. Advances in actinobacterial proteomics. *Chinese Journal of Biotechnology,* 30**,** 1044-1058.